THE ADAPTABILITY OF EMPIRICAL EQUATIONS TO CALCULATE POTENTIAL EVAPOTRANSPIRATION AND TREND ANALYSIS OF HYDROCLIMATOLOGICAL PARAMETERS FOR AGRICULTURAL AREAS IN NEWFOUNDLAND

by

K V G S PERERA

A Thesis Submitted to the

School of Graduate Studies

In partial fulfilment of the requirements for the degree of

Master of Science in Boreal Ecosystems and Agricultural Sciences

School of Science and the Environment

Grenfell Campus

Memorial University of Newfoundland

April, 2021

Corner Brook, Newfoundland

Abstract

Calculation of potential evapotranspiration (PET) has been problematic in Newfoundland (NL) due to the lack of measured data. Therefore, PET data obtained from the Pacific Field Corn Association for *St John's*, NL was compared against five empirical PET calculation equations (i.e. (i) radiation-based Priestley-Taylor (PT), and Makkink (M), (ii) temperature-based Hargreaves-Samani (HS), and Turc (T), and (iii) location-based Hamon (H)). Evaluation based on the results concluded that the HS equation would be appropriate to calculate PET in NL. Further calibrations and validations were done to modify the HS to better calculate PET for the growing season (May-October) in NL. The modifications improved the Root Mean Square Error (RMSE), Nash-Sutcliffe Efficiency (NSE) and co-efficient of determination (R^2) of the validated data. Trend assessment carried out using Innovative Trend Analysis (ITA) and Mann-Kendal (MK) tests indicated that both methods were in par with each other. Most of the significant positive trends of monthly total precipitation (0.375-2.210 mm/month/year) were available for September and October. Positive trends for minimum and maximum temperatures were found mostly concentrated within August and September with increments ranging from 0.015 to 0.062 ºC/month/year. PET trends of magnitudes up to 0.011 mm/month/year were observed mostly within September and October. Total water balance did not show as many positive trends as other parameters considered. However, the available positive trends (ranging from 0.018 to 0.076 mm/month/year) were also focused mostly within September. As a conclusion, the HS equation with modifications and error margins (where necessary) can be used to calculate PET accurately for the growing season in NL, and positive trends are observed mostly within the later periods of the growing season. The results of this study could be used in consideration of agricultural expansion, selecting cropping systems and water management systems of NL in future.

General Summary

Agricultural industry in Newfoundland (NL) can be threatened by fluctuations caused by climate change on total precipitation (PPT), potential evapotranspiration (PET) and total water balance. As a preliminary supportive attempt to address this issue, this study focused on selecting and modifying a suitable substitute PET calculation equation to be used instead of the commonly used Penman-Monteith equation. Secondly it was attempted to identify existing trends of PPT, maximum and minimum temperature, PET and total water balance and their magnitudes. Results revealed that the Hargreaves-Samani equation would be the most acceptable to calculate PET for the NL. The same equation was further modified to calculate PET values accurately for the growing season (May-October) in NL. Trend analysis carried out using Locally Weighted Scatterplot Smoothing (LOWESS), Mann-Kendal (MK), Innovative Trend Analysis (ITA) and Sen's Slope methods, indicated increasing PPT, PET, maximum and minimum temperatures and total water balance trends.

Acknowledgement

First and foremost, I would like to express my heartfelt gratitude to my family. Specifically, I want to thank my parents, my sister and other loved ones for their support and encouragement throughout this period.

I would like to extend my gratitude to my advisor Dr Lakshman Galagedara, for the guidance, encouragement and support given during the successful completion of this research. I am very grateful for his knowledge, patience and unerring ability to keep me on the right track. I would like to express my special thanks to my co-supervisor Dr Olga Vasilyeva and committee member Dr Adrian Unc, for sharing their broad knowledge and for the valuable comments and discussions.

I would like to express my utmost appreciation to Dr Chandra Jayasena for his guidance, encouragement, and the insight he gave on technical aspects of the research and in preparing manuscripts of this research.

Furthermore, I acknowledge the Environment Canada and the Pacific Field Corn Association (farmwest.com) for the raw data and available PET data. Graduate fellowship of Boreal Ecosystems and Agricultural Sciences Programs and Seed Money from the Memorial University of Newfoundland is much appreciated.

I especially thank my friends and colleagues, Mr Gnanakaran Maheswaran and Mr Jiaxu Wu, who have helped me in various aspects of this research.

All your support and cooperation are much appreciated.

Table of Contents

List of Tables

List of Figures

List of Appendices

List of Abbreviations and Symbols

b_{Sen} - Sen's Slope

D - ITA statistical indicator

Δ - Slope of the saturation vapor pressure vs. temperature curve

ESAT - Saturated vapour pressure at a given temperature

FAO - Food and Agriculture Organization

G - Sensible heat exchange from the surface to the soil

γ - Psychrometric constant

H - Hamon

HS - Hargreaves-Samani

ITA – Innovative Trend Analysis

λ - Latent heat of vaporization

Ld - Daytime length

M - Makkink

Max - Maximum

Min - Minimum

MK - Mann-Kendal test

n - number of data points

NL - Newfoundland

NSE - Nash-Sutcliffe Efficiency

PET - Potential Evapotranspiration

PFCA - Pacific Field Corn Association

PM - Penman-Monteith

PPT - total precipitation

PT - Priestley-Taylor

R^2 - Correlation coefficient

RHOSAT - Saturated vapour density

RMSE - Root Mean Square Error

Rn - Net radiation flux at the surface

Rs - Solar radiation

T – Turc

T_{max} - Maximum Temperature

T_{mean} – Mean Temperature

T_{min} - Minimum Temperature

WMO - World Meteorological Organization

$Z_{\alpha/2}$ - Confidence coefficient

σ - Population standard deviation

Chapter 1: Introduction

1.1 Overview

Studies show that the global climate is changing due to many reasons, anthropogenic activity being one cause (Mehan et al., 2016). Hydrological behaviours, whether it be on a local, regional, or global scale, are greatly influenced by weather extremes and climate changes (Gleick, 1989) and have become a primary concern of every country of the world. These weather extremes change the hydrological cycle affecting many necessary actions from agricultural practices to primary scale power generation (Mehan et al., 2016). Total precipitation (PPT) and potential evapotranspiration (PET) are the two most important natural water transfer processes between the atmosphere and land of the global water cycle. They are also the two most important natural factors governing rainfed agriculture. As the population of the world continues to grow, the food demand will also undeniably increase. Hydrological aspects hold much leverage in addressing this food demand through increased and sustained agricultural yield. Hence, it is essential to study the behaviours of precipitation and evapotranspiration extensively (Lu et al., 2005).

The government of Newfoundland and Labrador has planned to increase food production from a current 10% to 20% by 2022, and have decided to expand the land area for farms and cultivation by converting 64000 ha of forest area to farmlands (Government of Newfoundland and Labrador, 2017; Fisheries and Land Resources, 2017). To support this goal of the provincial government, it is imperative to calculate PET and water balance for potential agricultural areas in Newfoundland (NL). Even though there are research outcomes on PPT, and PET, and resultant water balance for the entire boreal region (King et al., 2018), there is little research focusing on hydrological aspects, including water balance, related to agricultural areas in NL. Also, identification of possible trends of hydroclimatological parameters would

support decision making such as the selection of the most suitable crops and cropping systems to sustain the agriculture industry.

The Food and Agriculture Organization (FAO) recommends that the Penman-Monteith (PM) equation be used for PET calculations. However, it is quite challenging to use this method as there are no or very few weather data available for NL. It is possible to use assumptions for parameters used in PM calculations. These assumptions may not be suited for every location in NL, which in return could result in errors in PM calculations, as each assumption made for each parameter may change the outcome of the PM calculation, rendering PM equation unreliable to calculate PET in NL. Therefore, it is crucial to select a method that will give reasonably accurate values as the PM equation using fewer parameters and assumptions in the calculation. Thus, results could be used for better agricultural practices as well as any other field where the involvement of PPT and PET parameters are vital.

1.2 Statistical Calculation of Potential Evapotranspiration

PET is the maximum allowed evaporation amount when there is an unlimited supply of water to evaporate. In other words, it is the amount of water that could evaporate from a particular land surface due only to the atmospheric demand (Lu et al., 2005; Penman, 1948; Thornthwaite, 1948). Even though measuring potential evaporation is feasible, it is not the same for the case of transpiration. This task is very complicated when there is scarce data, which leads to a lack of reliable calculations (Valipour et al., 2017). Hence, in most instances, empirical equations are used with certain assumptions to calculate PET for a given locality.

As many statistical methods are available to calculate PET, it is difficult to specify one method to be the most accurate and precise (Chen et al., 2005; Lang et al., 2017; Lu et al., 2005). Therefore, researchers have carried out many studies at various locations under different weather conditions to compare various PET calculation methods (Amthor et al., 2001; Grace

& Quick, 1988; Kisi, 2016; Kisi & Alizamir, 2018). The PM equation was suggested as the standard PET estimation equation by considering aerodynamic and physiologic parameters (Allen et al., 1998) by the FAO and World Meteorological Organization (WMO). PM produces accurate results for the PET because it is a combined equation of surface energy balance and radiation and considers many parameters such as net radiation, soil heat flux and specific heat of the air. As the standard method, PM equation can be used in most localities of the world without having to amend the equation (Allen, 2005).

However, as many meteorological parameters might not be measured or estimated especially in developing countries or less populated regions, an issue arises when calculating the PET using the PM equation because it utilises many meteorological parameters (Alkaeed et al., 2006; Venkataraman et al., 2016). Many researchers have studied other statistical methods or models to be used instead of the PM that would produce similar results. It should be noted that the equation selected to substitute PM in different studies would not always be the same due to prevailing weather, climatic, land-use conditions over the studied area. Some examples from previous studies are given as follows.

The temperature-based Thornthwaite equation was recommended as a substitute for PET calculation in Itoshima Peninsula Area, Fukuoka, Japan (Alkaeed et al., 2006). Makkink equation was identified as the best performing equation in the east Tibetan Plateau, yearly, and seasonally. In contrast, the Hargreaves-Samani equation showed an excellent performance along with Abtew and Makkink in summer and autumn in the arid river valley, southwest China (Lang et al., 2017). Priestley-Taylor, Penman and Shuttleworth equations were recommended to calculate PET in arid regions in northwest China (Li et al., 2016). Priestley-Taylor, Hamon and Turc methods were recommended for south-eastern Unites States (Lu et al., 2005). Hargraves-Samani equation was suggested as one of the suitable substitute models to calculate PET for all climatic regions of Iran (Raziei & Pereira, 2013). Priestley-Taylor and Turc

methods performed superior to the Penman-Monteith for estimating PET for various land covers in Florida (Douglas et al., 2009). Priestley-Taylor and Makkink were ranked as top models in accuracy for PET calculations for Switzerland (Xu & Singh, 2002). From a study caried out in Canada and Western Europe, it was noted that Baier-Robertson equation was suitable for PET calculation in Canada and Turc equation was suitable for Western Europe (Seiller & Anctil, 2016).

From the literature, it is possible to note that in such a scenario where data is scarce, each PET calculation equation performs differently in each situation. Therefore, to adapt a suitable substitute for PM to a given location, it is necessary to compare different equations with PM at a localised scale.

1.3 PPT, Minimum and Maximum Temperature, PET and Water Balance Trend Identification

Trend identification of PPT, maximum (max) and minimum (min) temperatures, PET and total water balance, is crucial as it provides a somewhat comprehensive understanding about the land to atmospheric water transfer (Katul & Novick, 2009). In return, this understanding can be effectively used in agricultural management, including estimating soil water supply and understanding drought or excess water availability (Park et al., 2018). Trend detection is also vital to understand the impacts of climate change over the hydrologic regime (Karpouzos et al., 2010).

Trends of hydroclimatological parameters differ from one another due to various factors such as location, ecosystem, climatic region, and degree of anthropogenic activity. For instance, a downward trend of PPT was observed from a study carried out in the Pieria regions of Greece (Karpouzos et al., 2010). In southern Italy an overall decreasing trend in PPT over 1923-2000 was detected with significantly different seasonal trends (Piccarreta et al., 2004). Partal &

Kahya, in 2006 indicated a noticeable decrease in the annual mean PPT, mostly in western and southern Turkey. The trend of meteorological parameters with Mann-Kendall trend analysis revealed a seasonal and monthly variability in Kolkata, India (Chaudhuri & Dutta, 2014). A study caried out over Canada indicated that the Prairies had become warmer and drier over a period from 1949 to 1989 (Gan, 1998). The annual max, min and mean temperature significantly increased over the Yangtze River Basin, China (Cui et al., 2017). There was no detectable PET trend in Chott-Meriem region of Tunisia (Mansour et al., 2017). A positive PET trend in the pan-arctic region was also reported (Zhang et al., 2009). Positive multi-decadal trends were identified in global terrestrial PET from 1981 to 2012 (Zhang et al., 2016). Therefore, it is imperative to identify trends in each of these components, viz: PPT, max and min temperatures and PET on a local scale to support the NL government's initiative to increase fresh food produce.

1.4 Objectives

The objective of this study focused on distinguishing a suitable method for local level PET calculation, to be used instead of the PM method for selected locations in NL. The selected methods for comparison were (i) radiation-based Priestley-Taylor (PT), and Makkink (M), (ii) temperature-based Hargreaves-Samani (HS), and Turc (T), and (iii) location-based Hamon (H). Once a suitable equation was selected to estimate PET within NL, modification to the equation was carried out to further finetune the calculation results to match PET in the growing season (May-October) in NL.

The second objective of this study was to identify and obtain an understanding of existing trends in PPT, max and min temperature, PET and water balance in each of the selected study locations, namely, *Cormack, Corner Brook, Cow Head, Deer Lake, Gander, Port Aux Basque, St John's* and *Stephenville*.

1.5 Structure of the thesis

This thesis follows a manuscript format and consists of three overall chapters.

Chapter 1: An introductory chapter to this research, including objectives, and structure of the thesis.

Chapter 2: A standalone manuscript highlighting the selection process of a suitable equation to replace FAO recommended PM. Results of multiple equation comparison with the PM and further modification of a selected substitute equation are presented. Application of the selected equation to all study locations are also illustrated.

Chapter 3: A second standalone manuscript describing trend analysis of total precipitation, maximum and minimum temperatures, potential evapotranspiration and total water balance using several trend identification methods commonly used in hydrology.

Chapter 4: Includes the general summary of the entire thesis and future recommendations to further progress the research.

1.6 References

Alkaeed, O., Flores, C., Jinno, K., & Tsutsumi, A. (2006). Comparison of several reference evapotranspiration methods for Itoshima Peninsula area, Fukuoka, Japan. *Memoirs of the Faculty of Engineering, Kyushu University*, *66*(1), 1-14.

Allen, R. (2005). Penman–Monteith equation.

Allen, R. G., Pereira, L. S., Raes, D., & Smith, M. (1998). FAO Irrigation and drainage paper No. 56. *Rome: Food and Agriculture Organization of the United Nations*, *56*(97), e156.

Amthor, J. S., Chen, J. M., Clein, J. S., Frolking, S. E., Goulden, M. L., Grant, R. F., ... & Wofsy, S. C. (2001). Boreal forest CO_2 exchange and evapotranspiration predicted by nine ecosystem process models: Intermodel comparisons and relationships to field

measurements. *Journal of Geophysical Research: Atmospheres*, *106*(D24), 33623-33648.

Chaudhuri, S., & Dutta, D. (2014). Mann–Kendall trend of pollutants, temperature and humidity over an urban station of India with forecast verification using different ARIMA models. *Environmental Monitoring and Assessment*, *186*(8), 4719-4742.

Chen, D., Gao, G., Xu, C. Y., Guo, J., & Ren, G. (2005). Comparison of the Thornthwaite method and pan data with the standard Penman-Monteith estimates of reference evapotranspiration in China. *Climate Research*, *28*(2), 123-132.

Cui, L., Wang, L., Lai, Z., Tian, Q., Liu, W., & Li, J. (2017). Innovative trend analysis of annual and seasonal air temperature and rainfall in the Yangtze River Basin, China during 1960–2015. *Journal of Atmospheric and Solar-Terrestrial Physics*, *164*, 48-59.

Douglas, E. M., Jacobs, J. M., Sumner, D. M., & Ray, R. L. (2009). A comparison of models for estimating potential evapotranspiration for Florida land cover types. *Journal of Hydrology*, *373*(3-4), 366-376.

Fisheries and Land Resources. (2017, December 14). Retrieved December 29, 2018, from https://www.releases.gov.nl.ca/releases/2017/ffa/1214n02.aspx

Gan, T. Y. (1998). Hydroclimatic trends and possible climatic warming in the Canadian Prairies. *Water Resources Research*, *34*(11), 3009-3015.

Gleick, P. H. (1989). Climate change, hydrology, and water resources. *Reviews of Geophysics*, *27*(3), 329-344.

Government of Newfoundland and Labrador. (2017). *The Way Forward*.

Grace, B., & Quick, B. (1988). A comparison of methods for the calculation of potential evapotranspiration under the windy semi-arid conditions of southern Alberta. *Canadian*

Water Resources Journal, *13*(1), 9-19.

Karpouzos, D. K., Kavalieratou, S., & Babajimopoulos, C. (2010). Trend analysis of precipitation data in Pieria Region (Greece). *European Water*, *30*(30), 30-40.

Katul, G., & Novick, K. (2009). Evapotranspiration. *Encyclopedia of Inland Waters*, 661-667.

King, M., Altdorff, D., Li, P., Galagedara, L., Holden, J., & Unc, A. (2018). Northward shift of the agricultural climate zone under 21st century global climate change. *Scientific Reports*, *8*(1), 1-10.

Kisi, O. (2016). Modeling reference evapotranspiration using three different heuristic regression approaches. *Agricultural Water Management*, *169*, 162-172.

Kisi, O., & Alizamir, M. (2018). Modelling reference evapotranspiration using a new wavelet conjunction heuristic method: wavelet extreme learning machine vs wavelet neural networks. *Agricultural and Forest Meteorology*, *263*, 41-48.

Lang, D., Zheng, J., Shi, J., Liao, F., Ma, X., Wang, W., ... & Zhang, M. (2017). A comparative study of potential evapotranspiration estimation by eight methods with FAO Penman–Monteith method in southwestern China. *Water*, *9*(10), 734.

Li, S., Kang, S., Zhang, L., Zhang, J., Du, T., Tong, L., & Ding, R. (2016). Evaluation of six potential evapotranspiration models for estimating crop potential and actual evapotranspiration in arid regions. *Journal of Hydrology*, *543*, 450-461.

Lu, J., Sun, G., McNulty, S. G., & Amatya, D. M. (2005). A Comparison of six potential evapotranspiration methods for regional use in the southeastern United States 1. *JAWRA Journal of the American Water Resources Association*, *41*(3), 621-633.

Mansour, M., Hachicha, M., & Mougou, A. (2017). Trend analysis of potential

evapotranspiration case of Chott-Meriem region (the Sahel of Tunisia). *International Journal of Agriculture Innovations and Research*, *5*, 703-708.

Mehan, S., Kannan, N., Neupane, R. P., McDaniel, R., & Kumar, S. (2016). Climate change impacts on the hydrological processes of a small agricultural watershed. *Climate*, *4*(4), 56.

Park, C. E., Jeong, S. J., Joshi, M., Osborn, T. J., Ho, C. H., Piao, S., ... & Feng, S. (2018). Keeping global warming within 1.5 C constrains emergence of aridification. *Nature Climate Change*, *8*(1), 70-74.

Partal, T., & Kahya, E. (2006). Trend analysis in Turkish precipitation data. *Hydrological Processes: An International Journal*, *20*(9), 2011-2026.

Penman, H. L. (1948). Natural evaporation from open water, bare soil and grass. *Proceedings of the Royal Society of London. Series A. Mathematical and Physical Sciences*, *193*(1032), 120-145.

Piccarreta, M., Capolongo, D., & Boenzi, F. (2004). Trend analysis of precipitation and drought in Basilicata from 1923 to 2000 within a southern Italy context. *International Journal of Climatology: A Journal of the Royal Meteorological Society*, *24*(7), 907-922.

Raziei, T., & Pereira, L. S. (2013). Estimation of ETo with Hargreaves–Samani and FAO-PM temperature methods for a wide range of climates in Iran. *Agricultural Water Management*, *121*, 1-18.

Seiller, G., & Anctil, F. (2016). How do potential evapotranspiration formulas influence hydrological projections?. *Hydrological Sciences Journal*, *61*(12), 2249-2266.

Thornthwaite, C. W. (1948). An approach toward a rational classification of climate. *Geographical Review*, *38*(1), 55-94.

Valipour, M., Sefidkouhi, M. A. G., & Raeini, M. (2017). Selecting the best model to estimate potential evapotranspiration with respect to climate change and magnitudes of extreme events. *Agricultural Water Management*, *180*, 50-60.

Venkataraman, K., Nelson, M., & Frandsen, C. (2016). Comparison of two temperature-based methods of estimating potential evapotranspiration (PET) in Texas. In *World Environmental and Water Resources Congress 2016* (pp. 699-708).

Xu, C. Y., & Singh, V. P. (2002). Cross comparison of empirical equations for calculating potential evapotranspiration with data from Switzerland. *Water Resources Management*, *16*(3), 197-219.

Zhang, K., Kimball, J. S., Mu, Q., Jones, L. A., Goetz, S. J., & Running, S. W. (2009). Satellite based analysis of northern ET trends and associated changes in the regional water balance from 1983 to 2005. *Journal of Hydrology*, *379*(1-2), 92-110.

Zhang, Y., Peña-Arancibia, J. L., McVicar, T. R., Chiew, F. H., Vaze, J., Liu, C., ... & Pan, M. (2016). Multi-decadal trends in global terrestrial evapotranspiration and its components. *Scientific Reports*, *6*(1), 1-12.

Co-authorship statement

A manuscript based on Chapter 2, entitled "The adaptability of empirical equations to calculate potential evapotranspiration for agricultural areas: A case study from Newfoundland, Canada" is expected to be submitted to The Journal of Water and Climate Change. K. V. G. S. Perera, the thesis author was the primary author, and Dr L. W. Galagedara (supervisor), was the corresponding and the senior author. Dr H. A. H. Jayasena, Dr A. Unc (committee member), and Dr O. Vasilyeva (co-supervisor) were the second, third and fourth authors, respectively.

For the work in Chapter 2, the design of the study was developed and carried out by Mr Perera with input from Dr Galagedara. Mr Perera was responsible for the data collection, analysis, and interpretation and writing of the manuscript. Dr Galagedara provided specific guidance on statistical analysis, data interpretation and the manuscript writing. Drs. Unc and Vasilyeva provided inputs for the statistical analysis, data interpretation and manuscript editing. Dr. Jayasena assisted in refining the manuscript and the methodology.

Chapter 2: The adaptability of empirical equations to calculate potential evapotranspiration for agricultural areas: A case study from Newfoundland, Canada.

2.1 Abstract:

Calculation of potential evapotranspiration (PET) has been a problem, due to the unavailability of measured meteorological data in Newfoundland. Hence, this study focused on selecting a suitable empirical equation which could be used in calculating PET under data-scarce scenarios. Daily PET values were calculated for selected agriculture-based eight different localities, including *Cormack, Corner Brook, Cow Head, Deer Lake, Gander, Port Aux Basque, St John's* and *Stephenville*, in Newfoundland, Canada, using measured weather data. Five empirical equations: Priestley-Taylor (PT), Makkink (M), Hargreaves-Samani (HS), Turc (T), and Hamon (H) were used to calculate PET and were compared with respective PET data available from the Pacific Field Corn Association, *St John's*, Newfoundland calculated based on Penman-Monteith (PM) method. The analysis indicated that the HS was the best method suited to calculate PET at *St John's* based on correlation coefficient (R^2= 0.970), a root-mean-square error (RMSE =0.242 mm/day), and a Nash-Sutcliffe Efficiency (NSE =0.944). Using data from *St John's* in Newfoundland, further statistical analyses, calibrations and validations were done to modify the HS to better approximate the PET for the growing season (May-October). The modifications improved the RMSE (0.069 mm/day), NSE (0.996) and R^2 (0.997) during the validation, and the modified HS was applied to other study locations. It was concluded that the temperature-based HS could be used as an adequate substitute for PM to calculate PET for Newfoundland. Based on the study results, this method is even recommended for remote locations in the world where accurate PET data are not available.

Keywords: Potential evapotranspiration; Hargreaves-Samani; Penman-Monteith; Turc; Hamon; Makkink; Priestley-Taylor; Newfoundland

2.2 Introduction

Weather extremes and climate change significantly influence the surface and subsurface hydrological behaviours from local pedon scale to global scales (Gleick, 1989; Vereecken et al., 2019). Such extreme events eventually lead to quantitative and qualitative deviations to the different components of the hydrological cycle. The ultimate adverse effects badly interfere with the vital sectors in the economy, causing declining agricultural production due to unpredicted water supply and power generation (Mehan et al., 2016). Total precipitation (PPT) and potential evapotranspiration (PET) are two critical components of the water cycle. They are the only natural means of water transfer between the atmosphere and the land. PET is the maximum allowed evapotranspiration (mm/day) when there is an unlimited water supply to evaporate from the ground and transpire through vegetation (Rind et al., 1990). In other words, the amount of water that could evaporate and transpire from a particular land surface depends only on the atmospheric demand (Lu et al., 2005; Penman, 1948; Thornthwaite, 1948). While measuring potential evaporation using instruments is feasible (Karlsson & Pomade, 2013), the measurement or calculation of transpiration is much more complex and involved with uncertainties as it varies with temporal stages of crop growth (Valipour et al., 2017).

Consequently, PPT and PET are the most decisive hydrological factors governing the output of rainfed agriculture. Therefore, understanding the spatial and temporal kinetics of PPT and ET is a crucial prerequisite under variable climatic conditions (Lu et al., 2005). Though long-term PPT, PET, and water balance data are available for the entire boreal region (King et al., 2018), the resolution was not adequate to take better agricultural decisions. Such inadequate

spatial resolution of PET/PPT data strongly interferes with the efficient water management decisions.

Under “The Way Forward” programme, the government of Newfoundland and Labrador expects to double the local food production to satisfy 20% of the provincial food requirements by 2022 (Government of Newfoundland and Labrador, 2017). Such initiatives have given the mandate for effective water resources management under rainfed agriculture which could maximise the land and water productivity. In achieving such goals, policy and decision-makers need to understand the crucial inputs of hydrological aspects. To maintain sustainability and to support the increased agricultural production, a suitable method for calculation of PET and then predict water balance for agriculturally potential regions in Newfoundland (NL) is essential. Hence, usage of empirical equations, which are commonly applicable under certain assumptions, to calculate PET for given localities is very important. Such equations include but are not limited to Penman-Monteith (PM), Makkink (M), Priestley-Taylor (PT), Hargreaves-Samani (HS), Turc (T), and Hamon (H).

Given many options for calculating PET (Zeleke & Wade, 2012), it is difficult to simply adopt one equation as accurate and precise for an allotted location (Chen et al., 2005; Lang et al., 2017; Lu et al., 2005). Comparisons of PET equations have been previously carried out under various weather and soil conditions for different regions (Grace & Quick, 1988; Kisi, 2016; Kisi & Alizamir, 2018; Li et al., 2016). However, as an accepted standard method that produces accurate results, the FAO recommends that PM equation can be used in most localities throughout the world without amending it (Allen, 2005). This may not be true when measured, or estimated weather parameters are sparsely available, viz; developing countries or less populated localities (Venkataraman et al., 2016; Alkaeed et al., 2006). As a result, scientists turn to other empirical equations such as T, that utilises temperature data, H, based on day length or HS, relies upon temperature and solar radiation, as a substitute for the PM equation.

This study focused on evaluating an empirical equation which could replace the data-driven PM equation for calculation of PET over agricultural regions in NL. The equations selected for this study include: (i) radiation-based PT and M; (ii) temperature-based HS, and T; and (iii) location-based H.

2.3 Methodology

2.3.1 Study locations and data collection

Locations for the present study were identified from the land use map of NL, where each location was selected as close as possible to agricultural areas, viz: *Cormack, Corner Brook, Cow Head, Deer Lake, Gander, Port Aux Basque, St John's* and *Stephenville*. Among these, *Cow Head, Port Aux Basque, St John's*, and *Stephenville* lie within coastal areas whereas *Corner Brook* and *Deer Lake* are associated with Humber river valley in Western NL. *Gander* resides close to the *Gander* lake, and *Cormack* is located further inland more towards the agricultural hinterlands (Figure 2-1).

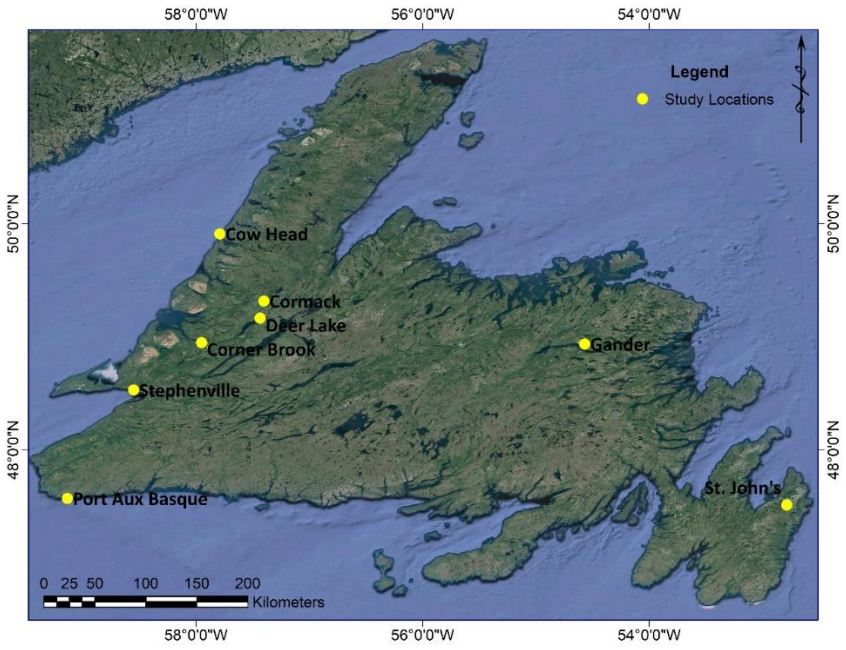

Figure 2-1: Terrain representation of Newfoundland, Canada including the selected study locations.

Daily total PPT and temperature (minimum-Min and maximum-Max) data for each location (Table 2-1) were extracted from the Environment Canada weather station network (Environment and Climate Change Canada, 2018).

Table 2-1: Summary of coordinates and elevation data of the selected study locations

Location	**Coordinates**		
	Latitude (N)	**Longitude (W)**	**Elevation (m)**
Cormack	49° 19’	57° 24’	153.9
Corner Brook	48° 57	57° 57’	4.6
Cow Head	49° 54’ 42”	57° 47’ 20”	15.2
Deer Lake	49° 13’	57° 24’	21.9
Gander	48° 56’ 47”	54° 34’ 37”	151.2
Port Aux Basque	47° 34’ 26”	59° 09’ 17”	39.7
St John’s	47° 37’ 20”	52° 44’ 34”	140.5
Stephenville	48° 32’	58° 33’	24.7

2.3.2 Determination of a replacement to the PM equation

Five different empirical equations were used to calculate PET, and the results were evaluated using already available PET data (Table 2-2). Since daily Min and Max temperatures and PPT data were readily available, other parameters such as net radiation, vapour pressure, and day length used in each equation were separately calculated as per the procedures described in (Allen et al., 1998) and (Zotarelli et al., 2010).

Among the selected stations in NL, estimated PET data based on the PM equation were readily available only for the *St John’s* station from 2014 to 2017 at the Pacific Field Corn Association-PFCA (Evapotranspiration, 2018). Yet, these PM data was also subjected to assumptions during calculations (Et calculation, 2018) and a complete metadata set was not accessible. Since there were no other measured evapotranspiration data available for the region in question, the accuracy of the PET calculations (using above five equations) was evaluated by comparing

with the PET data estimated using the PM equation for the *St John's* station acquired by the PFCA.

2.3.3 Calibration, validation, and application of the empirical equation

Once a suitable equation was selected, a series of calculation procedures were adapted, as illustrated in the flowchart (Figure 2-2). The selected equation was subjected to a further modification (calibration) by adjusting the equation constants using the MS solver function to accurately calculate the PET. The term "modified", as used henceforth in this paper, refers to the optimised equation by changing the constants for the *St John's* dataset. The modification of the equation was done explicitly focusing on the growing season (May-October) in NL to accurately obtain a specific equation to calculate PET in the said growing season. By doing so, this modified equation could be used to support decisions and development regarding agricultural water management in NL.

As dictated by common practice, from the four years of available PET data obtained from PFCA, three years of May to October data (2014-2016) was used to calibrate the selected PET equation. The remaining PET data for May-October of 2017 was then used to validate the modified equation. The resulting data set calculated from the modified PET equation from 2014 through 2016 is referred to as the calibration set. The data calculated for 2017 is referred to as the validation set throughout this study. Once the validation was completed with acceptable accuracy, the modified PET calculation equation was applied to other study locations within the growing season (May-October). For locations in NL, where the modified equation was planned to be applied, a margin of error was incorporated (Eq. 2-6).

$$Margin\ of\ error = \pm Z_{\alpha/2}.\frac{\sigma}{\sqrt{n}} \quad (2\text{-}6)$$

Where $Z_{\alpha/2}$ was the confidence coefficient, σ referred to the population standard deviation, and n was the number of data points. As the margin of error depends on σ (Helsel & Hirsch, 2002),

the criterion for applying the best selected empirical equation for a different study location hinged upon whether the variances between averaged temperatures of the study location and *St John's* differed significantly from each other.

Table 2-2: Empirical equations used in the study.

No	Equation	Formula	Remarks
2-1	Priestley-Taylor (PT) (Priestley & Taylor, 1972)	$PET = \frac{1}{\lambda}\frac{\Delta(Rn - G)}{(\Delta + \gamma)}\alpha$	$\alpha = 1.26$ $\lambda = 2.45\ MJ/kg$
2-2	Makkink (M) (Valipour et al., 2017)	$PET = C1\frac{1}{\lambda}\frac{\Delta Rs}{(\Delta + \gamma)} - C2$	$\lambda = 2.45$, C1 = 0.61 and C2 = 0.12
2-3	Turc (T)-1961 (Lu et al., 2005)	$PET = C1\ (\frac{T_{mean}}{T_{mean}+C2})(Rs + C3)$	Rs must be in mm/day. Hence, Rs in MJ/m^2/day is divided by 2.45. C1 = 0.0133, C2 = 15°C and C3 = 50 MJ/m^2/day
2-4	Hargreaves-Samani (HS) (Hargreaves & Samani, 1982, Hargreaves & Samani, 1985)	$PET = C1\frac{Ra}{\lambda}\ (T_{max} - T_{min})^{PC}(T_{mean} + C2)$	Ra must be in mm/day. Hence, Ra in MJ/m^2/day is divided by 2.45. C1 = 0.0023, C2 = 17.8 and PC = 0.5
2-5	Hamon (H)-1963 (Lu et al., 2005)	$PET = C1(Ld)(RHOSAT)(KPEC)$	$RHOSAT = 216.7\ x\ \frac{ESAT}{(T_{mean} + 237.3)}$ $ESAT = 6.108\ exp^{\left(\frac{17.26939\ (T_{mean})}{(T_{mean}+237.3)}\right)}$ $KPEC = 1.2$ C1 = 0.1651

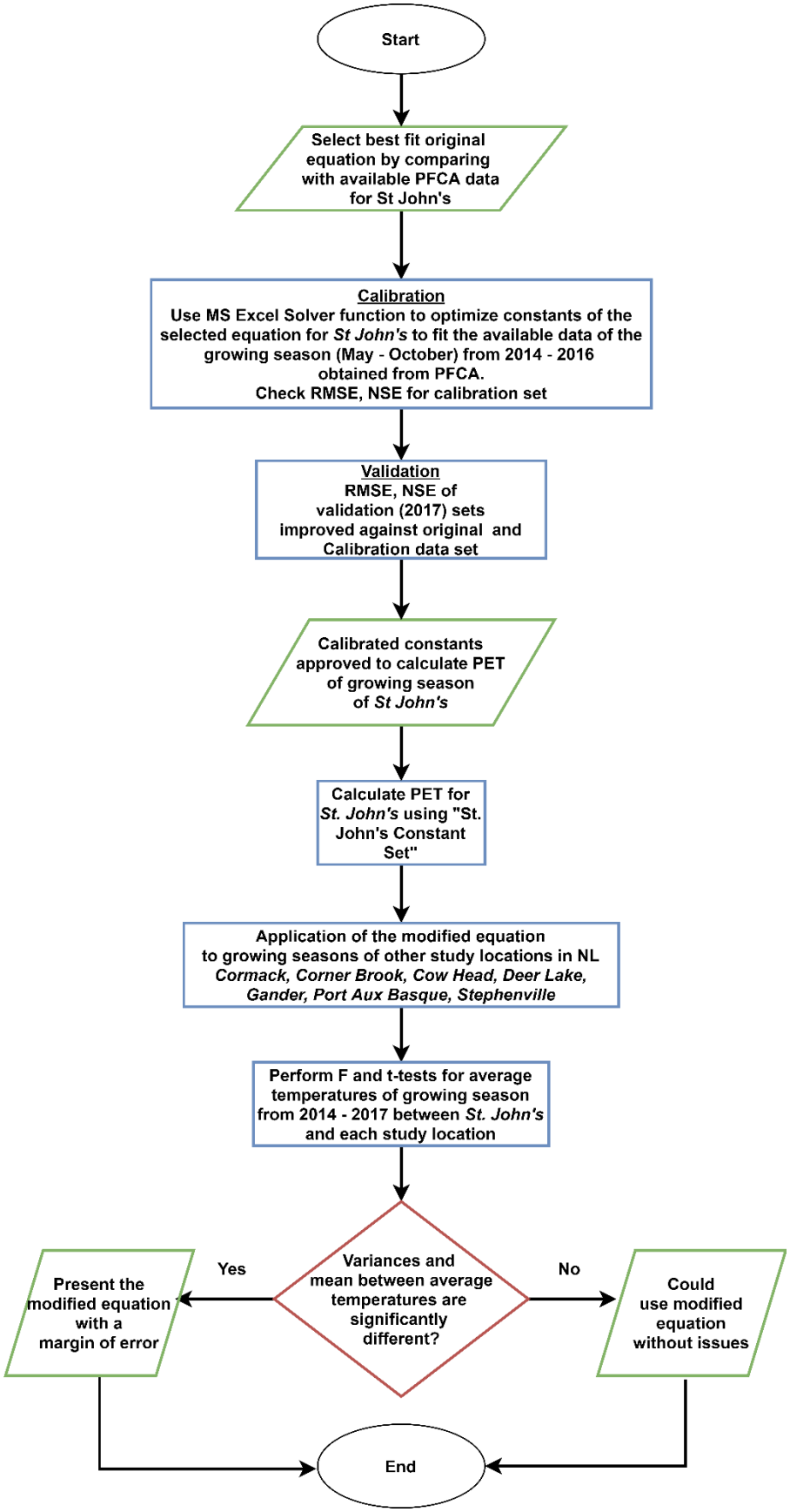

Figure 2-2: Methodology flowchart of modifying the selected empirical equation (HS) and application procedure to study locations in Newfoundland.

2.3.4 Statistical analysis

To select the most suitable empirical equation and to evaluate the accuracy of the calibration and validation of the modified PET equation, the following statistical analyses were completed and utilised. Statistical analyses were carried out to establish the correlation, the slope and intercept comparisons (deviation from the 1:1 line) between the calculated PET data and the PFCA PET data complying with the methods described by Zaiontz (2019). Additionally, Root Mean Square Error (RMSE), Student's t-test and Nash Sutcliff Efficiency (NSE) (AgriMetSoft, 2018; Nash & Sutcliffe, 1970) were further employed to evaluate the accuracy and the performance of each PET calculation equation. The goal was to identify the empirical equation with the least RMSE, an NSE close or equal to 1, and a probability of t-test above 0.05. Further, the slope and intercept values of each empirical equation were also considered in assessing the performance of each equation. Additionally, F-tests were carried out to calculate if the variance between two parameters significantly differed from each other as a supporting statistical test to be used before calculating the margin of error. The α threshold was assumed at 0.05 (95% probability) for all statistical analysis.

2.4 Results and Discussion

2.4.1 Comparison of Potential Evapotranspiration (PET) with Pacific Field Corn Association (PFCA)

The results were obtained through subsequent attempts performed as described in the following paragraphs. This attempt was focused on *St John's*, NL to identify an empirical equation that could calculate the PET values closer to PFCA data without having to utilise many hydrometeorological parameters. The correlations between PET calculated by each equation and PFCA data are represented in Figure 2-3. Figure 2-3 additionally incorporates linear trend lines to provide a clear relationship between each calculated and the PFCA data for *St John's*,

viz; how much the calculated data deviated from the available data (deviation from the 1:1 line). The HS correlated better with PFCA data with an R^2 value of 0.970 (Figure 2-3(d)). In the case of H equation, it showed an R^2 value of 0.796 with PFCA data (Figure 2-3(e)). Even though it was not as accurate as HS equation when comparing with the 1:1 line, it was possible to observe that H equation produced better fits than PT, M or T equations for *St John's* (Figure 2-3(a, b, c)).

The statistical results (RMSE, NSE and student t-test) and the linear regression by comparing with the 1:1 line for the selected empirical equations against the PFCA data are summarised in Table 2-3. The HS equation had a slope of 1.115 and an intercept of -0.114 mm/day with an RMSE of 0.242 mm/day and an NSE of 0.944. The PT, M and T equations did not provide better statistical correlations to PFCA data. They highly overestimated the calculated PET compared to HS and H. The p-values of student t-test revealed that PET calculated by all equations except for HS ($p = 0.102$) was significantly different from PET values of PFCA data of *St John's*. Results revealed that the HS equation performed very well when compared to other PET calculation equations tested for *St John's*.

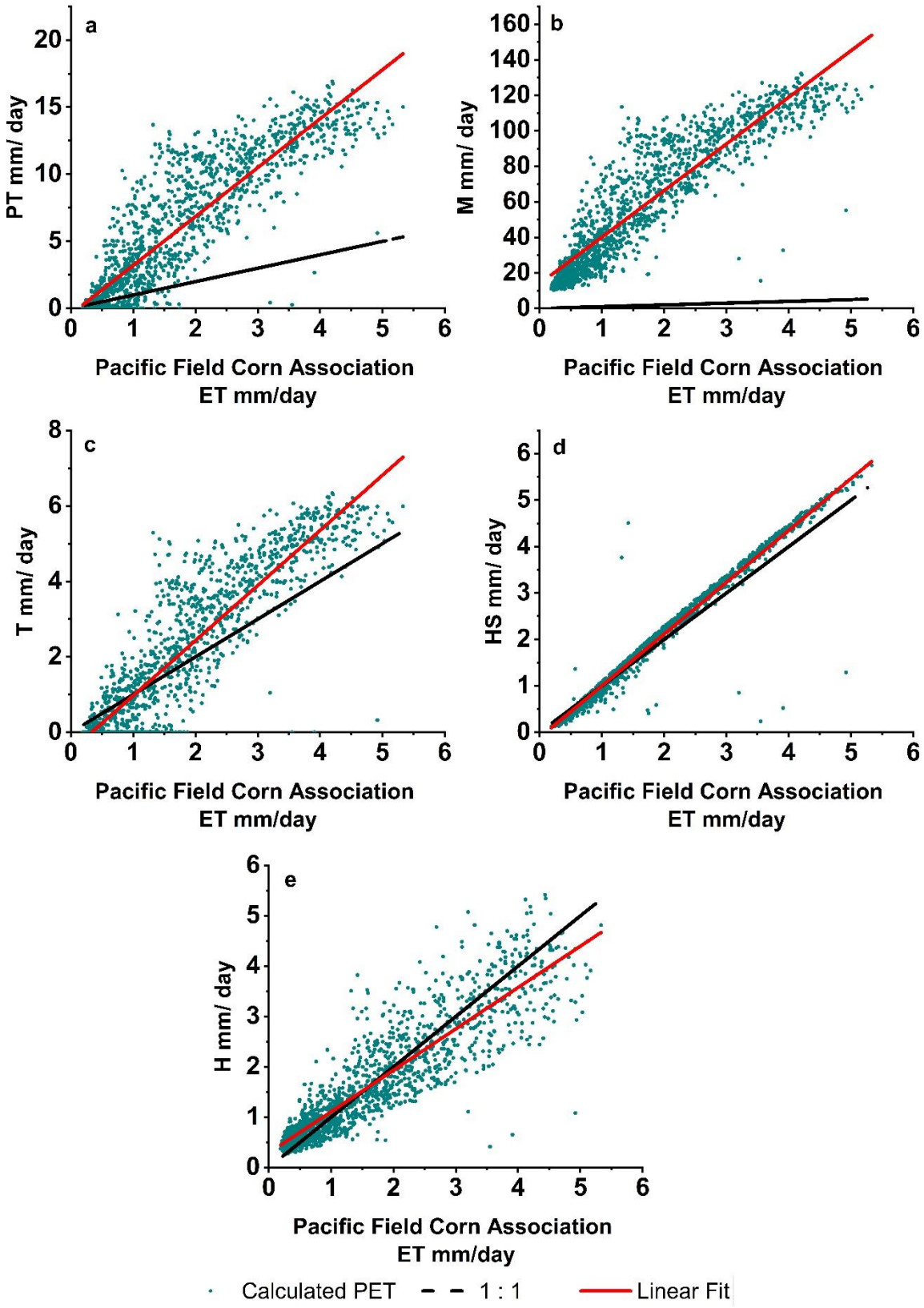

Figure 2-3: Scatter plot of calculated potential evapotranspiration (PET) against Pacific Field Corn Association (PFCA) for St John's. a: Priestley and Taylor (PT) (R^2 = 0.790); b: Makkink (M) (R^2 = 0.829); c: Turc (T) (R^2 = 0.818); d: Hargreaves-Samani (HS) (R^2 = 0.970); e: Hamon (H) (R^2 = 0.796)

Table 2-3: Summary of slope and intercept analysis of potential evapotranspiration (PET) calculated using different equations and PET data available from Pacific Field Corn Association (PFCA) for St John's (α = 0.05)

PET Equation	Slope	Intercept (mm/day)	RMSE (mm/day)	P-value of Student T-test	Nash-Sutcliffe Coefficient
PT	3.642[S]	-0.433[S]	2.316	0.000	-20.04
M	26.247[S]	13.921[S]	14.702	0.000	-2861.867
T	1.460[S]	-0.487[S]	0.851	0.000	0.26
HS	**1.115[S]**	**-0.114[S]**	**0.242**	**0.102**	**0.944**
H	0.822[S]	0.287[S]	0.513	0.795	0.795

S-the slope (or the intercept) of the calculated data is significantly different from the 1:1 slope (or the intercept).

The comparisons that were carried out revealed that HS can be used as a suitable substitute for PET calculation in the *St John's* location. Being a temperature-based equation, HS provides an additional advantage since the min and max temperature data are available for almost all locations, even in the rural areas. Though the T is also a temperature-based equation, it contains a solar radiation component. Due to lack of data, it had to be assumed that the actual duration of sunlight was equal to total daylight hours, causing less accurate results from this equation. Whereas H, being a location-based equation, relying mainly on the day length, performed moderately to HS. When considering PT and M, these equations also carry solar radiation component in the calculation procedures, which, as mentioned above, was based on assumptions. This might have led to the poor performance given by PT and M.

2.4.2 Calibration and validation of HS to better calculate Potential Evapotranspiration.

Calibration and validation results of HS based on comparisons carried out for *St John's* are presented in a stepwise manner as follows. Based on the statistical analysis for *St John's*

constant set, tested against available data from PFCA, (Table 2-4) an improved RMSE (0.165 mm/day), and NSE (0.977) was obtained during the calibration. Moreover, the validation set resulted in an RMSE of 0.069 mm/day and NSE of 0.996, showing further improvement of the HS compared to the un-modified and the calibrated data sets.

Table 2-4: Summary of statistical comparison of modified Hargreaves-Samani (PET–HS) calculated for St John's using St John's constant set against respective Pacific Field Corn Association (PFCA) data (α = 0.05)

Location		**RMSE**	**R^2**	**NSE**	**1:1 Analysis Slope**	**1:1 Analysis Intercept**
St John's	HS	0.315	0.976	0.916	S	NS
	Calibrated - HS	0.165	0.979	0.977	NS	NS
	Validated - HS	0.069	0.997	0.996	NS	NS

S-Significantly different; NS-not significant

A graphical representation of the comparison between the PFCA data and HS values and the validation set for the growing season (May-October 2017) obtained by modification as mentioned above, is given in Figure 2-4. The validation set obtained by the modification of HS provided PET values slightly less than that of the original un-modified HS equation which confirmed that the un-modified HS overestimates values for *St John's*. Thus, the HS calculated using *St John's* constant set performed as the best compared to the un-modified HS**.** Therefore, the modified HS took the form as given in Eq. 2-7.

$$PET = 0.0018 \frac{Ra}{\lambda} (T_{max} - T_{min})^{0.5411} (T_{mean} + 19.6605) \quad \text{Eq. 2-7}$$

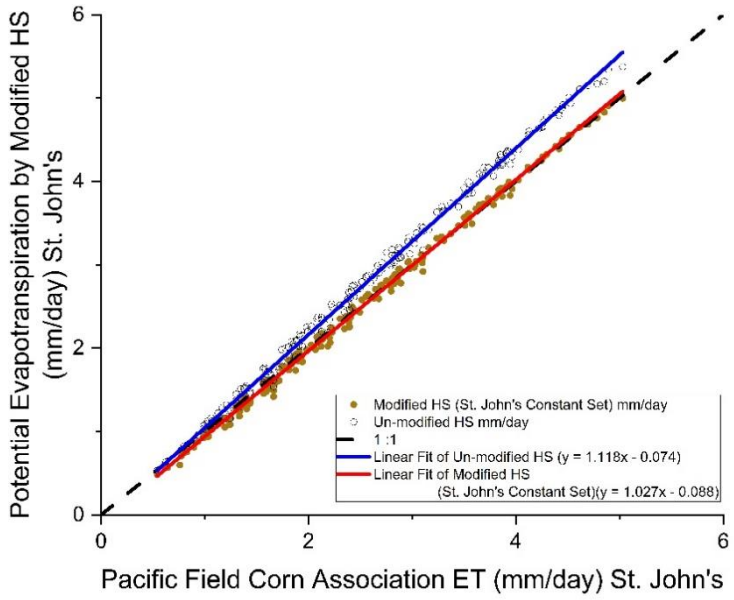

Figure 2-4: Validation of calculated potential evapotranspiration (PET) (May-October 2017) using modified HS using St John's (R^2 = 0.997) constants with respect to original un-modified (R^2 = 0.996) HS by comparing with Pacific Field Corn Association (PFCA) data

2.4.3 Application of the modified HS equation

The statistical results of F and t-tests of average temperatures of the remaining study locations compared to the average temperature of *St John's* are given in Table 2-5. The variance and the mean of the averaged temperatures of *St John's* were not significantly different (P > 0.05) for *Cormack, Deer Lake* and *Gander*. Additionally, the variances of the average temperature of *Corner Brook* were also not significantly different, but the mean was different from that of *St John's*. Therefore, the modified HS as a temperature-based method, could be directly used for PET calculation for *Cormack, Corner Brook, Deer Lake* and *Gander.*

For the remaining locations, viz: *Cow Head, Port Aux Basque* and *Stephenville* that had a significant variability from the *St John's* location, the modified HS was applied with a margin of error as given in Table 2-5. A graphical representation of the temporal variation of the estimated PET using the modified HS is given in Figure 2-5. The lower and upper bounds of

95% margin of error were given only to those study locations where the modified HS could not be applied directly.

Table 2-5: Statistical results of F and t-tests of mean temperature comparison data of study locations against St. John's mean temperature data, and summary of error margins for 95%, 90% and 80% confidence levels for three locations in Newfoundland where the modified Hargreaves-Samani (PET–HS) equation of St. John's cannot be directly applied.

Location	Probability of F test	F - test against St. John's	Margin of error (mm/day)		
			95% Confidence level	90% Confidence level	85% Confidence level
Cormack	0.203	NS	-	-	-
Corner Brook	0.380	NS	-	-	-
Cow Head	0.005	S	0.072	0.060	0.053
Deer Lake	0.313	NS	-	-	-
Gander	0.141	NS	-	-	-
Port Aux Basque	0.000	S	0.055	0.046	0.041
Stephenville	0.000	S	0.071	0.059	0.052

Even though HS was initially designed for the California dry climate (Lu et al., 2005), it appeared that HS, with certain modifications, could be used as a suitable substitute to calculate PET in NL as well. The analysis carried out in this study for the locations in NL proved that the HS, in both unmodified and modified forms, performed better than other equations considered. The results of this paper also agree that HS could be used successfully in Newfoundland Boreal ecozone, as well as in most of other climate and ecoregions. For example, Valipour and Eslamian (2014) considered HS equation (with modifications) to be a suitable substitute for calculating PET in most provinces of Iran. Similar results were found for localities throughout Iran where HS equation was recommended to be utilised as a substitute for FAO recommended PM equation (Raziei & Pereira, 2013; Sepaskhah & Razzaghi, 2009). Additionally, our study results fell in line with Martinez-Cob & Tejero-Juste (2004), where it has shown that the HS equation worked well for semi-arid windy locations in Spain. Unlike in

the case of Xu & Singh (2002), where a modified PT and M equations closely resembled pan evaporation of Changins, Switzerland, these equations highly overestimated PET values for the study locations of the current study. The present findings of this study also contradicted the outcomes of Lu et al. (2005) which preferred PT, T and H equations, as PT and T highly over-estimates PET values in all the locations in this study when compared to available data. Results from this study also differed from that of Seiller & Anctil, (2016), where Baier-Robertson equation was mentioned as suitable for PET calculation in Canada.

Even though, H performed better than PT and T; HS was proven to be a better substitute to calculate PET in NL in previous sections of this study.

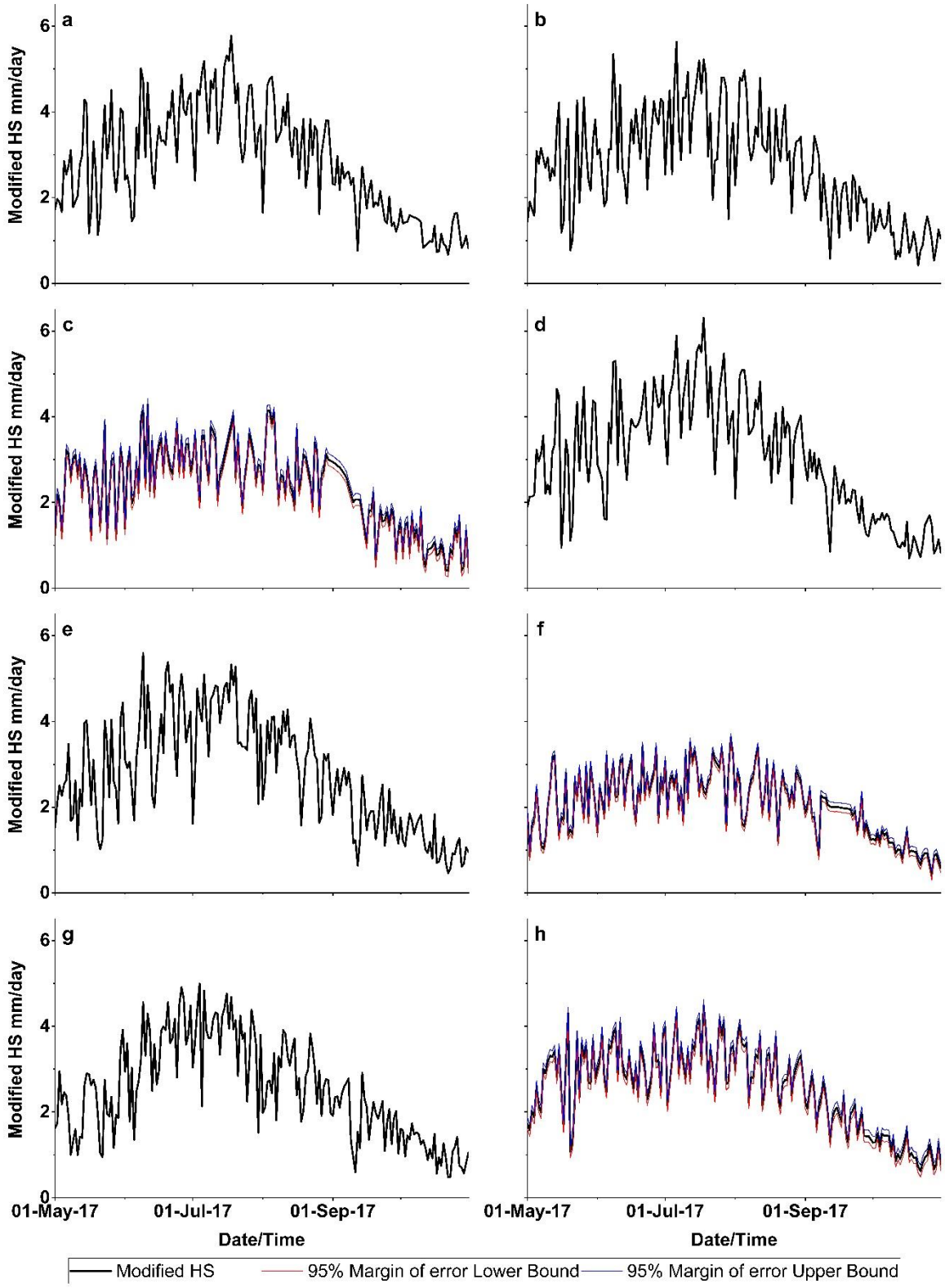

Figure 2-5: Temporal variation of the potential evapotranspiration (PET) calculated using the modified Hargreaves-Samani (HS) for the growing season (May-October) of 2017 for eight selected locations in Newfoundland. Upper and lower bounds of error margins are given to locations where modified HS cannot be applied directly. a: Cormack; b: Corner Brook; c: Cow Head; d: Deer Lake; e: Gander; f: Port Aux Basque; g: St John's; h: Stephenville

2.5 Conclusion

It was concluded that out of the tested equations, the temperature-based HS equation could be used as an adequate substitute for FAO recommended PM equation to calculate PET for the NL. The selected modified HS equation could be applied to calculate PET during the growing season for study locations of *Cormack*, *Corner Brook*, *Deer Lake* and *Gander*. For other locations (*Cow Head*, *Port Aux Basque*, and *Stephenville*), the same modified HS equation could be used with an error margin provided for each location.

When PET calculations are needed in NL for decisions on agricultural water management, cropping systems, integrated watershed management, and water balance and hydrological modelling, this modified HS equation can be used with reasonable accuracy.

The method can be recommended for remote locations in the world where accurate PET data are not available. It could provide low-cost data for making adaptation decisions and to improve agricultural water management, wetland and pond performances or even hydrologic modelling aiming at sustainable production systems.

A comparative study of real-time measured PET data with remote sensing-based inputs and water balance prediction is advised as a progressive next step.

2.6 Acknowledgement

The authors would like to acknowledge the Environment Canada and the Pacific Field Corn Association (farmwest.com) for the raw data and available PET data. Graduate fellowship of Boreal Ecosystems and Agricultural Sciences Programs and Seed Money from the Memorial University of Newfoundland is much appreciated.

2.7 References

AgriMetSoft. (2018). Nash Sutcliffe model efficiency coefficient. Retrieved August 20, 2018, from https://agrimetsoft.com/calculators/Nash Sutcliffe model Efficiency coefficient

Alkaeed, O., Flores, C., Jinno, K., & Tsutsumi, A. (2006). Comparison of several reference evapotranspiration methods for Itoshima Peninsula area, Fukuoka, Japan. Memoirs of the Faculty of Engineering, Kyushu University, 66(1), 1-14.

Allen, R. (2005). Penman–Monteith equation.

Allen, R. G., Pereira, L. S., Raes, D., & Smith, M. (1998). FAO Irrigation and drainage paper No. 56. Rome: Food and Agriculture Organization of the United Nations, 56(97), e156.

Chen, D., Gao, G., Xu, C. Y., Guo, J., & Ren, G. (2005). Comparison of the Thornthwaite method and pan data with the standard Penman-Monteith estimates of reference evapotranspiration in China. Climate Research, 28(2), 123-132.

Environment and Climate Change Canada. (2018). Historical Data. Retrieved October 4, 2018, from https://climate.weather.gc.ca/historical_data/search_historic_data_e.html

Evapotranspiration. (2018). Farmwest. Retrieved October 25, 2018, from https://farmwest.com/climate/calculators/evapotranspiration/#DailyData

Et Calculation. (2018). Farmwest. Retrieved October 30, 2018, from https://farmwest.com/climate/calculator-information/et/et-calculation/

Gleick, P. H. (1989). Climate change, hydrology, and water resources. Reviews of Geophysics, 27(3), 329-344.

Government of Newfoundland and Labrador. (2017). The Way Forward.

Grace, B., & Quick, B. (1988). A comparison of methods for the calculation of potential evapotranspiration under the windy semi-arid conditions of southern Alberta. Canadian Water Resources Journal, 13(1), 9-19.

Hargreaves, G. H., & Samani, Z. A. (1982). Estimating potential evapotranspiration. Journal of the Irrigation and Drainage Division, 108(3), 225-230.

Hargreaves, G. H., & Samani, Z. A. (1985). Reference crop evapotranspiration from temperature. Applied Engineering in Agriculture, 1(2), 96-99.

Helsel, D. R., & Hirsch, R. M. (2002). Statistical methods in water resources. USGS (p. 310). TWRI-4-A3.

Karlsson, E., & Pomade, L. (2013). Methods of estimating potential and actual evaporation. Salt Lake City: Department of Water Resources Engineering.

King, M., Altdorff, D., Li, P., Galagedara, L., Holden, J., & Unc, A. (2018). Northward shift of the agricultural climate zone under 21st century global climate change. Scientific Reports, 8(1), 1-10.

Kisi, O. (2016). Modeling reference evapotranspiration using three different heuristic regression approaches. Agricultural Water Management, 169, 162-172.

Kisi, O., & Alizamir, M. (2018). Modelling reference evapotranspiration using a new wavelet conjunction heuristic method: wavelet extreme learning machine vs wavelet neural networks. Agricultural and Forest Meteorology, 263, 41-48.

Lang, D., Zheng, J., Shi, J., Liao, F., Ma, X., Wang, W., ... & Zhang, M. (2017). A comparative study of potential evapotranspiration estimation by eight methods with FAO Penman–Monteith method in southwestern China. Water, 9(10), 734.

Li, S., Kang, S., Zhang, L., Zhang, J., Du, T., Tong, L., & Ding, R. (2016). Evaluation of six potential evapotranspiration models for estimating crop potential and actual evapotranspiration in arid regions. Journal of Hydrology, 543, 450-461.

Lu, J., Sun, G., McNulty, S. G., & Amatya, D. M. (2005). A Comparison of Six Potential Evapotranspiration Methods for Regional Use in the Southeastern United States 1. JAWRA Journal of the American Water Resources Association, 41(3), 621-633.

Martınez-Cob, A., & Tejero-Juste, M. (2004). A wind-based qualitative calibration of the Hargreaves ET0 estimation equation in semiarid regions. Agricultural Water Management, 64(3), 251-264.

Mehan, S., Kannan, N., Neupane, R. P., McDaniel, R., & Kumar, S. (2016). Climate change

impacts on the hydrological processes of a small agricultural watershed. Climate, 4(4), 56.

Nash, J. E., & Sutcliffe, J. V. (1970). River flow forecasting through conceptual models part I—A discussion of principles. Journal of Hydrology, 10(3), 282-290.

Penman, H. L. (1948). Natural evaporation from open water, bare soil and grass. Proceedings of the Royal Society of London. Series A. Mathematical and Physical Sciences, 193(1032), 120-145.

Priestley, C. H. B., & Taylor, R. J. (1972). On the assessment of surface heat flux and evaporation using large-scale parameters. Monthly Weather Review, 100(2), 81-92.

Raziei, T., & Pereira, L. S. (2013). Estimation of ETo with Hargreaves–Samani and FAO-PM temperature methods for a wide range of climates in Iran. Agricultural Water Management, 121, 1-18.

Rind, D., Goldberg, R., Hansen, J., Rosenzweig, C., & Ruedy, R. (1990). Potential evapotranspiration and the likelihood of future drought. Journal of Geophysical Research: Atmospheres, 95(D7), 9983-10004.

Seiller, G., & Anctil, F. (2016). How do potential evapotranspiration formulas influence hydrological projections?. Hydrological Sciences Journal, 61(12), 2249-2266.

Sepaskhah, A. R., & Razzaghi, F. (2009). Evaluation of the adjusted Thornthwaite and Hargreaves-Samani methods for estimation of daily evapotranspiration in a semi-arid region of Iran. Archives of Agronomy and Soil Science, 55(1), 51-66.

Thornthwaite, C. W. (1948). An approach toward a rational classification of climate. Geographical Review, 38(1), 55-94.

Valipour, M., & Eslamian, S. (2014). Analysis of potential evapotranspiration using 11 modified temperature-based models. International Journal of Hydrology Science and Technology, 4(3), 192-207.

Valipour, M., Sefidkouhi, M. A. G., & Raeini, M. (2017). Selecting the best model to estimate potential evapotranspiration with respect to climate change and magnitudes of extreme events. Agricultural Water Management, 180, 50-60.

Venkataraman, K., Nelson, M., & Frandsen, C. (2016). Comparison of two temperature-based methods of estimating potential evapotranspiration (PET) in Texas. In World Environmental and Water Resources Congress 2016 (pp. 699-708).

Vereecken, H., Weihermüller, L., Assouline, S., Šimůnek, J., Verhoef, A., Herbst, M., ... & Xue, Y. (2019). Infiltration from the pedon to global grid scales: An overview and outlook for land surface modeling. Vadose Zone Journal, 18(1), 1-53.

Xu, C. Y., & Singh, V. P. (2002). Cross comparison of empirical equations for calculating potential evapotranspiration with data from Switzerland. Water Resources Management, 16(3), 197-219.

Zaiontz, C. (2019). Real statistics using excel: Comparing the slopes for two independent samples. Retrieved March 22, 2019, from http://www.real-statistics.com/regression/hypothesis-testing-significance-regression-line-slope/comparing-slopes-two-independent-samples/

Zeleke, K. T., & Wade, L. J. (2012). Evapotranspiration estimation using soil water balance, weather and crop data. Evapotranspiration: remote sensing and modeling, 1, 41-58.

Zotarelli, L., Dukes, M. D., Romero, C. C., Migliaccio, K. W., & Morgan, K. T. (2010). Step by step calculation of the Penman-Monteith Evapotranspiration (FAO-56 Method). *Institute of Food and Agricultural Sciences. University of Florida*.

Co-authorship statement

A manuscript based on Chapter 3, entitled "Trend Analysis of Total Precipitation, Minimum and Maximum Temperature, Potential Evapotranspiration and Total Water Balance: A Case Study from Newfoundland" has been prepared to be submitted to a peer-reviewed journal. K. V. G. S. Perera; the thesis author was the primary author and Dr L.W. Galagedara (supervisor) was the corresponding and senior author. Dr A. Unc (committee member), Dr. H. A. H. Jayasena, and Dr O. Vasilyeva (co-supervisor) were second third and fourth authors respectively.

For the work in Chapter 3, the design of the study was developed and carried out by Mr Perera with input from Dr Galagedara. Mr Perera was responsible for the data collection, analysis, and interpretation and writing of the manuscript. Dr Galagedara provided specific guidance on statistical analysis, data interpretation and manuscript writing. Drs. Unc, Jayasena and Vasilyeva provided inputs for the statistical analysis, data interpretation and manuscript editing. Prof Jayasena assisted in refining the manuscript and the methodology.

Chapter 3: Trend analysis of total precipitation, minimum and maximum temperature, potential evapotranspiration, and total water balance: A case study from Newfoundland

3.1 Abstract

Ability to observe trends of a hydrological parameter is precious in hydrological studies with applications in agriculture, forestry, water resources management and many other applications. A study was conducted to detect general trends of total precipitation (PPT), minimum (min) and maximum (max) temperatures, potential evapotranspiration (PET) and total water balance for eight different agriculturally essential locations (i.e. *Cormack, Corner Brook, Cow Head, Deer Lake, Gander, Port Aux Basque, St John's and Stephenville)* within Newfoundland (NL). Weather data of 36 to 72 years, downloaded from Environment Canada, were used in this analysis. Innovative Trend Analysis (ITA) was applied to obtain such trends, along with the Mann-Kendal trend (MK) test and Sen's slope estimator to calculate the magnitude of significant trends. Moreover, comparison of the results of ITA and MK tests were found to be in par with each other. According to the MK and ITA tests, positive trends for min and max temperatures were observed mostly for August and September for almost all locations considered in this study with increments ranging within 0.015-0.062 C°/month/year. The PPT trends with magnitudes of 0.375-2.210 mm/month/year were found mostly within September and October. Additionally, PET trends closely followed max and min temperatures, with increments ranging up to 0.011 mm/month/year. Positive trends of total water balance (ranging 0.018-0.076 mm/month/year) were also focused mostly within September, and October. In conclusion, positive trends of PPT, PET, Min and Max temperatures and total water balance,

are available in the selected locations within the growing season. Such trends would have an impact on decisions making on agricultural expansion and practices in NL.

3.2 Introduction

Components of the hydrologic cycle are subjected to change throughout the globe (Prăvălie et al., 2019), and it is no different to the boreal regions as well (Fernandes et al., 2007). Total precipitation (PPT) and potential evapotranspiration (PET), are two critical components of the hydrological cycle (Mehan et al., 2016; Taylor et al., 2016), especially concerning agricultural or ecosystem hydrology. Nevertheless, it remains as one of the most challenging aspects to calculate PET due to changing environmental conditions and complex surface-atmospheric interactions (Zhang et al., 2011). Calculating PET and water balance and their trends have become highly important due to several factors such as agricultural water management and drought monitoring. These trends provide a somewhat comprehensive understanding of the land to atmospheric water transfer (Katul & Novick, 2009), including agricultural management and estimating soil water supply recommendation (Park et al., 2018). Unexamined PET measures or trends could give rise to potential drought or water surplus (Ghilain, 2016; Senay et al., 2015), both of which are negative extremes, for agricultural purposes and domestic water supply in particular.

The PET trends or patterns differ from one another, spatially and temporally due to various reasons. A short-scale PET study carried out in tropical South Asian rainforest ecosystems showed fluctuating or seasonal variations (Lim et al., 2009). Decreasing trends were found in China, involving the Yellow River; which has a temperate deciduous forest ecosystem (Zhang et al., 2011). Increasing trends of PET were found throughout the world as exemplified by many researches including King et al., (2018), Prăvălie et al., (2019) and Taylor et al., (2016). Sudden steep declining patterns in PET were also noticed, such as found in Central Valley,

California, which followed air temperature, dew point temperature and relative humidity trends (Szilagyi & Jozsa, 2018). As a response to the intensifying climate change, *i.e.* increasing temperature in the pan-arctic region had an overall PET increasing trend (Zhang et al., 2009). However, in Canada, there was an increasing trend of the PET in western and eastern coasts while having a mixed or decreasing PET trend for central and southern Canada (Fernandes et al., 2007; Zhang et al., 2009). If the boreal forests are considered, characterised by sub-arctic climate and approximately 50°-70° latitude in the Northern hemisphere, extending broadly through North American and Asian continents (Brandt, 2009; Larsen, 2013); the PET increased with time and the projected PET trends until 2099 also continued to rise (King et al., 2018).

To obtain an improved awareness of the PET trends, it is better to analyse a selected study area at a time in order to account for the spatial and temporal variation. Understanding such trends could be utilised for improved agricultural management practices, specifically in the said selected study area for more productive cultivation. In this research, it was attempted to study trends for selected locations, based on agricultural importance, on Newfoundland (NL). These study locations are namely, *Cormack, Corner Brook, Cow Head, Deer Lake, Gander, Port Aux Basque, St John's and Stephenville.* Trends of min and max temperatures, PPT, PET and total water balance were considered for this study focusing on the hypothesis that the trends of these parameters are increasing in NL. A modified Hargreaves-Samani (HS) equation (Eq 3-1) for the growing season (May - October) was used to calculate PET for study locations.

$$PET = 0.0018 \frac{Ra}{\lambda} (T_{max} - T_{min})^{0.5411} (T_{mean} + 19.6605) \quad \text{Eq. 3-1}$$

3.3 Methodology

3.3.1 Study Locations and Data

Eight agriculturally essential locations from the NL were selected as study locations for this research (Figure 3-1). The selection was made using croplands indications of land use maps of NL created using satellite images and ArcGIS software. The selected study locations and the duration of the data used at each location are given in Table 3-1.

The PPT and temperatures (min and max) data were downloaded for the above-mentioned study locations from the Environment Canada weather station network (Environment and Climate Change Canada, 2020). Missing data were filled using HEC-DSSVue (Hydrology Engineering Center - Data Storage System Visual Utility Engine). The total water balance was calculated as the difference of the PPT and PET. All calculations were carried out on a daily scale focusing on the growing season (May-October) in NL.

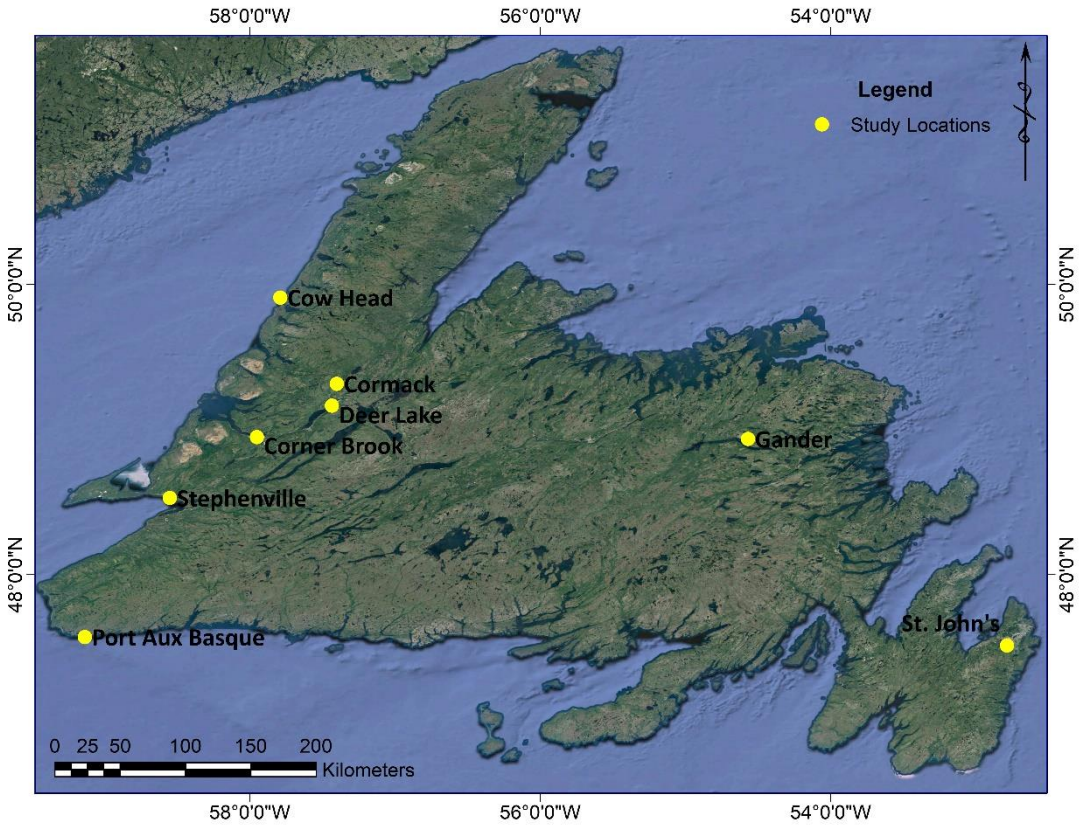

Figure 3-1: Terrain representation of Newfoundland, Canada including the selected study locations.

Table 3-1: Availability and duration of the temperature and total precipitation data

Location	Data Availability	Duration (years)
Cormack	1981-2019	39
Corner Brook	1947 - 2019	73
Cow Head	1983 - 2019	37
Deer Lake	1947-2019	73
Gander	1947-2019	73
Port Aux Basque	1956-2019	64
St John's	1947 - 2019	73
Stephenville	1947 - 2019	73

3.3.2 Study of existing trends

Time series of daily values of PPT, PET, max and min temperatures and water balance were plotted, and the variability was observed as an initial step. Due to the high variability, monthly averages of min and max temperatures, PET and total water balance were considered for further analysis following the common practice (Caloiero, 2017; Kisi, 2015; Kumar et al., 2017;

Mohorji et al., 2017). The PPT was considered as monthly totals. Three different statistical and graphical techniques were employed for trend detection and clarification. Any trends, peaks and troughs of the patterns of PPT, PET, max and min temperatures and water balance were explored using Locally Weighted Scatterplot Smoothing (LOWESS) (Chandler & Scott, 2011). As LOWESS analysis was based on graphically identifying trends, statistical trends of the monthly averaged min and max temperatures and the average monthly PET for the selected study locations were studied using Mann-Kendal trend (MK) test and Innovative Trend Analysis (ITA) (Şen, 2012). When compared to the MK test, ITA is a relatively new method for trend analysis (Kisi, 2015; Kisi & Ay, 2014; Kişi et al., 2018).

3.3.2.1 Mann-Kendal (MK) Test

The MK test is a non-parametric, rank-based trend recognition method designed to detect monotonous trends in a given time series data set. This method was used initially by Mann (1945), and the test statistic was later developed by Kendall (1975). This method is well used, more frequently than other non-parametric tests such as Sen's T or Spearman's rho, due to its simplicity and the broader scope of applicability (Tabari et al., 2011; Tosunoglu & Kisi, 2017; Wu & Qian, 2017). The S statistic of the MK test can be calculated as.

$$S = \sum_{i=1}^{n-1} \sum_{j=i+1}^{n} sign\,(x_i - x_j) \tag{3-2}$$

$$sign\,(x_i - x_j) = \begin{cases} if\ (x_i - x_j) < 0\ then - 1 \\ if\ (x_i - x_j) = 0\ then\ 0 \\ if\ (x_i - x_j) > 0\ then\ 1 \end{cases} \tag{3-3}$$

$$Var(S) = \frac{n(n-1)(2n+5) - \sum_{k=1}^{l} t_k(t_k-1)(2t_k+5)}{18} \tag{3-4}$$

$$Z = \begin{cases} if\ S < 0\ then\ \dfrac{S+1}{\sqrt{Var(S)}} \\ if\ S = 0\ then\ 0 \\ if\ S > 0\ then\ \dfrac{S-1}{\sqrt{Var(S)}} \end{cases} \quad (3\text{-}5)$$

Where in Equation (3-2), *n* is the length of the data set and x_i, and x_j denotes the data values at times *i* and *j*, respectively. Negative *S* value indicates a decrease in trend and vice versa for positive *S* values (Tosunoglu & Kisi, 2017). The statistical significance of the trend is calculated with no trend as the null hypothesis (H_0). If $n > 10$, the statistic *S* is assumed to be normally distributed with a mean of zero and a variance is calculated using Equation (3-4). l is the number of tied groups in the considered data set, and t_k is the number of data in the k^{th} tied group (Cui et al., 2017; Kisi, 2015; Partal & Kahya, 2006). In the absence of tied groups, the summation process of Equation (3-4) is neglected, and the standard *Z* statistic is computed, as shown in Equation (3-5) (Kisi & Ay, 2014). The test was carried out for 95% and 90% confidence levels (CL) using the R software's *'trend'* package (Pohlert, 2020).

3.3.2.2 Sen's slope estimator

To estimate the slope of the trend lines observed by the MK test, Sen's slope estimator was used. According to the method of Sen (1968), the magnitude of the slope of the trend can be estimated as given in Equation 3-6.

$$b_{Sen} = Median\left[\frac{y_i - y_j}{i - j}\right] \ \forall j < i \quad (3\text{-}6)$$

Where y_i and y_j are data at time points *i* and *j*, respectively. If there are *N* values in the time series, then one can get as many as *n = N(N-1)/2* slope estimates and b_{Sen} is taken as the median of these *n* values (Khaliq et al., 2009). The significance of the slope was accounted alongside MK test results, where Sen's slope was accepted for those instances where the *Z* value of the MK test was significant.

3.3.2.3 Innovative trend analysis (ITA) (Şen, 2012)

Usually, the most common methods used for trend analysis include and are not limited to MK test and Spearman's rho (Cui et al., 2017; Duhan & Pandey, 2013; Fu et al., 2013). Nevertheless, some assumptions are associated with this method, such as non-normality of distribution, independent structure of the time series, length of the data set and absence of serial correlation. It is also not possible to calculate the trend magnitude using these methods (Kisi, 2015; Şen, 2012). The foundation of the ITA is based on subsection time series plots retrieved from a selected time series data of interest on a cartesian coordinate system. The ITA method does not have restraining assumptions as MK or Spearman's rho tests, hence would be much reliable in trend analysis studies (Öztopal & Şen, 2017; Şen, 2012).

The ITA is carried out by dividing a time-series data into two halves, and the data in each half are rearranged in ascending order. The first half is then plotted on the X-axis of a cartesian coordinate system while the second half is plotted on the Y-axis. The basis of this trend analysis method is that two-time series are identical to each other, their plot against each other shows a scatter of points on the 1:1 line (Kisi & Ay, 2014; Şen, 2012). A time-series data is said to be with no trend if the plotted points fall on the 1:1 line. If the plots fall on the upper half on a straight line, it is said to have a monotonic increasing trend and if within the lower half, it is a monotonic decreasing trend. The closer the plotted points get to the 1:1 line, the trend magnitudes get weaker (Şen, 2017; Şen, 2012).

Furthermore, ITA has the ability to identify non-monotonic trends embedded within the same time series, whereas frequently used methods like MK; these variating trends may be hidden (Şen, 2012). It is also possible to detect low, mid and high trend regions of the time series with the ITA (Kisi & Ay, 2014). Even though the ITA is a qualitative measure, recent attempts have been made to quantify the trend given by the ITA method as well (Cui et al., 2017; Wu & Qian,

2017). A trend indicator *D* is introduced, which is calculated as shown in Equation 3-7, *n* is the number of observations of each sub-series and *x* is the average of the first half of the data set. Multiplication of 10 is due to bring the *D* value to the same scale as the MK test.

$$D = \frac{1}{n}\sum_{i=1}^{n}\frac{10\ (y_i - x_i)}{\bar{x}} \tag{3-7}$$

It is possible that ITA might give better trend analysis results than MK. Since the ITA method is relatively new, it was decided that ITA was to be carried out in conjunction with MK and LOWESS analysis in this study to acquire detailed trend analysis.

3.4 Results and Discussion

Monthly variations of each hydrometeorological parameter are given within the growing season for each location (Figure 3-2). The PPT showed a higher variation in October at *Cormack, Corner Brook, Port Aux Basque* and *St John's*, and it was high in July, August and September for the remaining locations. The max temperature variation was higher in May for all locations except *Port Aux Basque*. When the total 6-month (May-October) max temperature variation was considered, it was possible to identify *that Cow Head, Port Aux Basque* and *Stephenville* had relatively lower variations compared to the other locations. A notable min temperature variation was detected at *Deer Lake, Gander, Port Aux Basque* and *St John's*, where the variation was higher in July than the rest of the months. Higher variations of modified HS were noted at *Deer Lake* and *St John's* for May. A relatively lower variation within the total 6-months was also noted for *Cow Head, Port Aux Basque*, and *St John's,* that was similar in pattern to the max temperature. A possible reason for these temperature and modified HS variations might be the relative location and topography of the study areas. *Cow Head, Port Aux Basque* and *St John's* are coastal areas that are under higher influence of wind currents flowing over the ocean. Additionally, the effect of hurricanes on *St John's* is much higher than

other selected locations. Being located closer to a large water body might aid in moderating the temperature in these areas, which in return is reflected in modified HS. When concerning total water balance, all locations followed a similar pattern, where the range of the total water balance shifted towards the positive from May to October. A possible reason for this might be the gradually increasing PPT and decreasing modified HS from May to October.

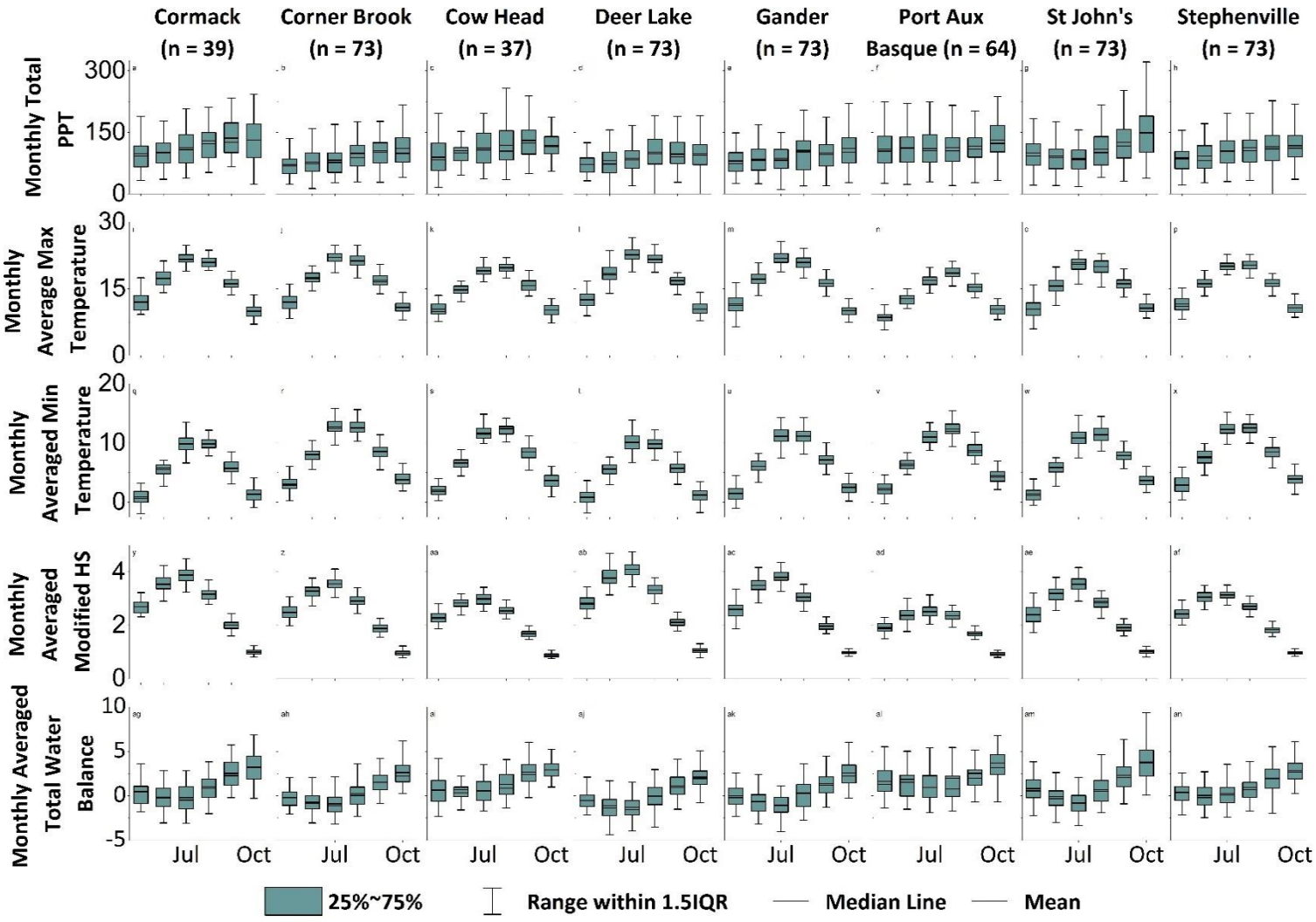

Figure 3-2: Box plots of monthly variations in PPT (mm), max and min temperatures (ºC), PET (mm/day) and total water balance (mm)

3.4.1 LOWESS trend analysis

Monthly time series analysis of PPT, min and max temperatures, modified HS and total water balance based on the LOWESS analysis are tabulated in Table 3-2 and illustrated in Figures 3-3 to 3-10. Standard deviations were also incorporated within the graphs for temperatures, PET, and total water balance, to observe the variation of each parameter from the LOWESS trend.

Table 3-2: LOWESS trend indication results

Month	Study Location	LOWESS trend indication				
		Total Monthly PPT	**Max Temperature**	**Min Temperature**	**Modified HS**	**Total Water Balance**
May	*Cormack*	No	No	No	No	No
	Corner Brook	No	Yes (+)	No	Yes (+)	No
	Cow Head	No	No	No	No	No
	Deer Lake	No	Yes (+)	No	Yes (+)	No
	Gander	Yes (+)	No	No	No	No
	Port Aux Basque	No	Yes (+)	Yes (+)	Yes (+)	No
	St John's	No	No	No	No	No
	Stephenville	No	Yes (+)	No	Yes (+)	No
June	*Cormack*	No	No	No	No	No
	Corner Brook	Yes (+)	Yes (+)	Yes (+)	No	No
	Cow Head	No	No	No	Yes (+)	No
	Deer Lake	No	No	No	Yes (+)	No
	Gander	Yes (+)	No	No	No	No
	Port Aux Basque	Yes (+)	Yes (+)	Yes (+)	Yes (+)	No
	St John's	No	No	No	No	No
	Stephenville	Yes (+)	Yes (+)	No	Yes (+)	No
July	*Cormack*	No	Yes (+)	No	Yes (+)	No
	Corner Brook	No	Yes (+)	Yes (+)	Yes (+)	No
	Cow Head	No	No	No	Yes (+)	No
	Deer Lake	No	Yes (+)	No	Yes (+)	No
	Gander	Yes (+)	No	No	No	No
	Port Aux Basque	No	Yes (+)	Yes (+)	Yes (+)	No
	St John's	Yes (+)	No	Yes (+)	Yes (+)	No
	Stephenville	No	Yes (+)	No	Yes (+)	No
August	*Cormack*	Yes (+)	Yes (+)	Yes (+)	Yes (+)	No
	Corner Brook	Yes (+)	Yes (+)	Yes (+)	Yes (+)	Yes (+)

	Cow Head	No	Yes (+)	Yes (+)	Yes (+)	No
	Deer Lake	Yes (+)	Yes (+)	No	Yes (+)	No
	Gander	No	Yes (+)	Yes (+)	Yes (+)	No
	Port Aux Basque	Yes (-)	Yes (+)	Yes (+)	Yes (+)	No
	St John's	No	Yes (+)	Yes (+)	Yes (+)	No
	Stephenville	Yes (+)	Yes (+)	Yes (+)	Yes (+)	No
September	*Cormack*	Yes (+)	No	Yes (+)	No	Yes (+)
	Corner Brook	Yes (+)	Yes (+)	Yes (+)	Yes (+)	Yes (+)
	Cow Head	Yes (+)	Yes (+)	Yes (+)	Yes (+)	Yes (+)
	Deer Lake	Yes (+)	Yes (+)	No	Yes (+)	Yes (+)
	Gander	Yes (+)	No	Yes (+)	No	No
	Port Aux Basque	No	Yes (+)	Yes (+)	Yes (+)	No
	St John's	No	Yes (+)	Yes (+)	Yes (+)	Yes (+)
	Stephenville	Yes (+)	Yes (+)	Yes (+)	Yes (+)	Yes (+)
October	*Cormack*	Yes (+)	No	No	Yes (+)	Yes (+)
	Corner Brook	Yes (+)	Yes (+)	Yes (+)	No	Yes (+)
	Cow Head	Yes (+)	Yes (+)	Yes (+)	Yes (+)	No
	Deer Lake	Yes (+)	Yes (+)	No	Yes (+)	Yes (+)
	Gander	Yes (+)	Yes (+)	No	No	No
	Port Aux Basque	Yes (+)	Yes (+)	Yes (+)	Yes (+)	No
	St John's	Yes (+)	Yes (+)	Yes (+)	No	No
	Stephenville	Yes (+)	Yes (+)	Yes (+)	Yes (+)	Yes (+)

Overall, positive trends were observed in all assessed parameters throughout all locations within August, September, and October. The month of September had positive PPT trends with exceptions of *Port Aux Basque* (Figure 3-8-e) and *St John's* (Figure 3-9-e). *Corner Brook, Gander, Port Aux Basque*, *St John's*, and *Stephenville* had positive PPT trends for June (Figures 3-4-b, 3-7-b, 3-8-b, 3-9-b, and 3-10-b). In all locations except *Gander* and *St John's*, there were no trends identified for all tested parameters for July. Positive trends of PPT in August were only identified for locations excluding *Cow Head*, *Gander* and *St John's* (Figures 3-5-d, 3-7-d and 3-9-d), whereas there was no trend in PPT of all locations for May.

Increasing max temperature trends were identified throughout all locations for August. Every location except *Cormack* displayed positive trends in max temperature for October (Figure 3-3-l). Positive trends were also observed for September for all locations except in *Gander* (Figure 3-7-k) and *Cormack* (Figure 3-3-k). *Cow Head, Gander* and *St John's* showed no trend pattern for July, whereas other locations had positive trends. Only *Corner Brook, Port Aux Basque* and *Stephenville* indicated positive trends for June (Figures 3-4-h, 3-8-h, and 3-10-h). The locations that showed a trend for June also showed positive trend patterns for May. *Deer Lake* also indicated increasing trends for May (Figure 3-6-g).

Trend patterns of min temperatures also behaved similarly to max temperature for August. The only positive trend identification for May was observed at *Port Aux Basque* (Figure 3-8-m), where other locations showed no trends. Both *Corner Brook* and *Port Aux Basque* indicated a positive trend in min temperature for June (Figures 3-4-h, and 3-8-h). Trends of min temperature for July was similar to that of June. *St John's* also showed increasing trends of min temperature for June as well (Figure 3-9-h). Min temperature trends for September was in all locations except *Cormack* and *Deer Lake*, whereas October also indicated no trends for *Cormack, Deer Lake* and *Gander*.

It was possible to notice that the modified HS trends mostly followed temperature trend patterns as expected, especially max temperature. All locations indicated positive trends for August, whereas for July and September only *Gander* did not show a PET trend (Figure 3-7-o and 3-7-q). For October, *Gander* and *St John's* did not show trends (Figures 3-7-r, and 3-4-r). Additionally, *Corner Brook* also indicated no trend for October (Figure 3-4-r). PET trends were observed at *Corner Brook, Deer Lake, Port Aux Basque* and *Stephenville* for May and June. Furthermore, *Cow Head* also had a positive trend indication for June (Figure 3-5-n).

Considering water balance; there was no trend indication in any location for June and July. *Stephenville* showed a less prominent positive trend for May (Figure 3-10-s), and *Corner Brook* showed a positive trend in August (Figure 3-4-v). In contrast, other locations did not show any trend for May and August, respectively. All locations excluding *Gander* and *Port Aux Basque* showed positive water balance trends for September. October showed positive trends for all locations except *St John's*. In general, September and October showed increasing water balance trend.

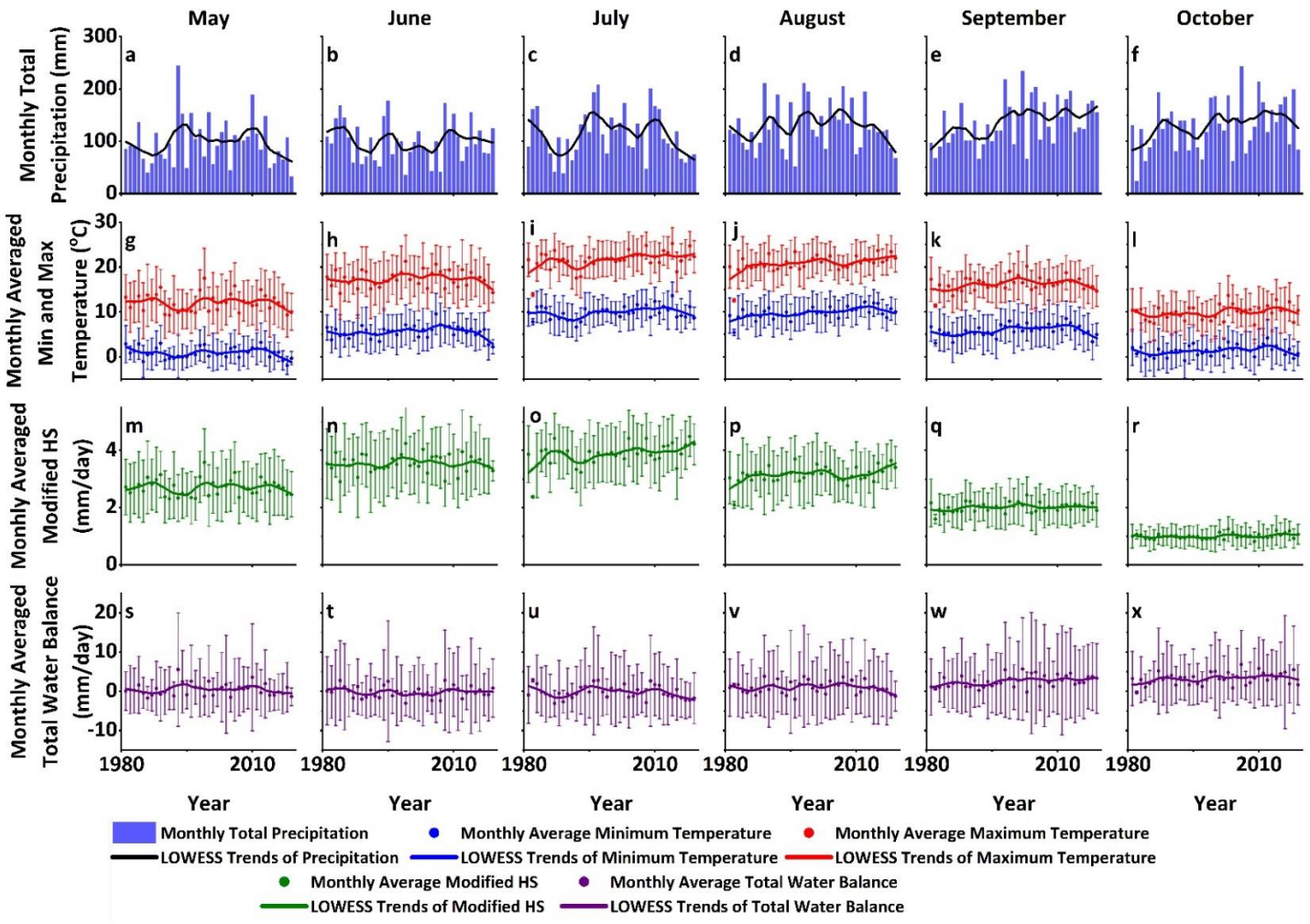

Figure 3-3: LOWESS trend analysis for Cormack with trends of monthly total precipitation, monthly averaged min and max temperatures, monthly averaged modified HS, and monthly averaged total water balance (standard deviations are given for temperatures, PET and total water balance, No of Years = 39).

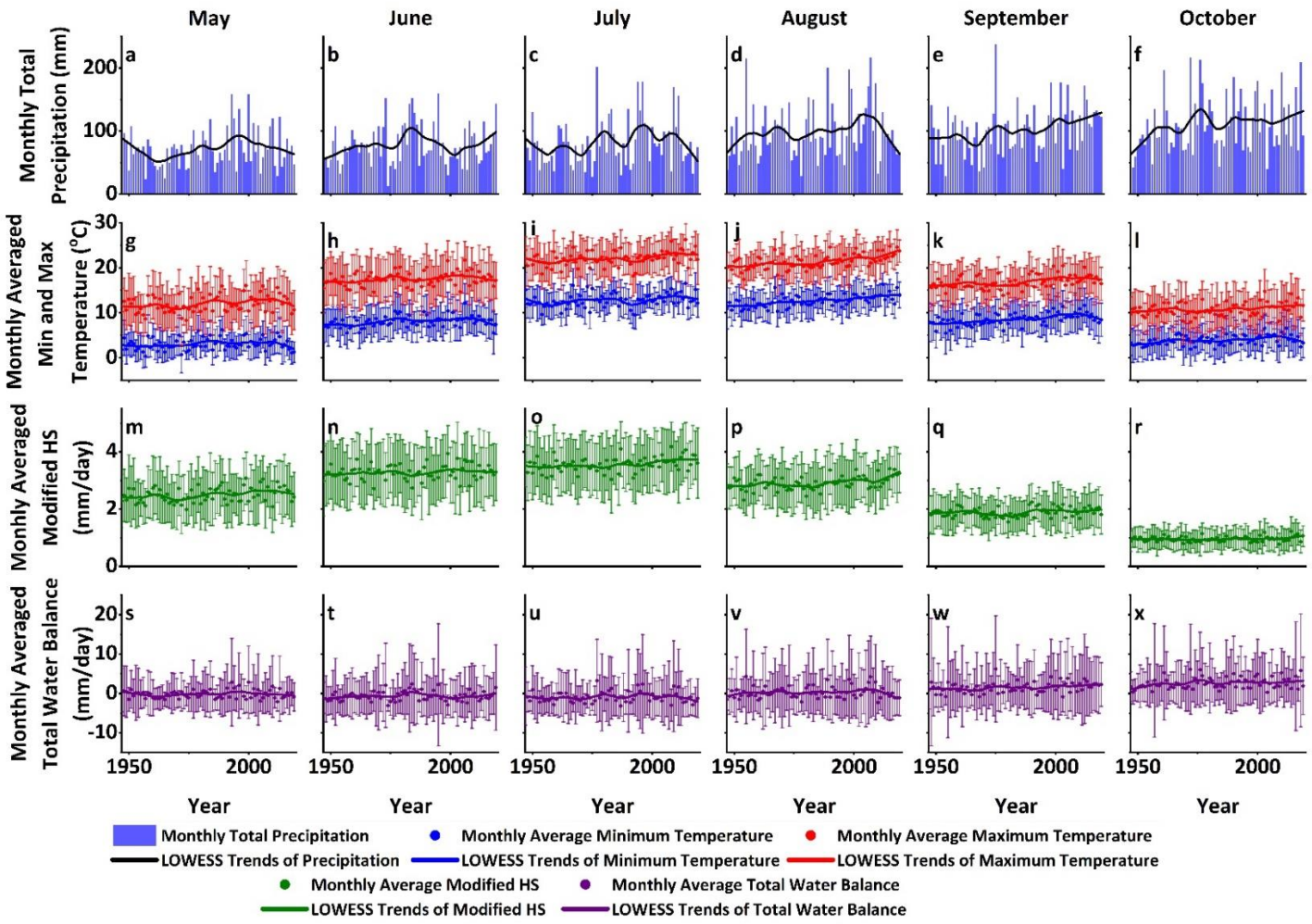

Figure 3-4: LOWESS trend analysis for Corner Brook with trends of monthly total precipitation, monthly averaged min and max temperatures, monthly averaged modified HS and monthly averaged total water balance (standard deviations are given for temperatures, PET and total water balance, No of Years = 73).

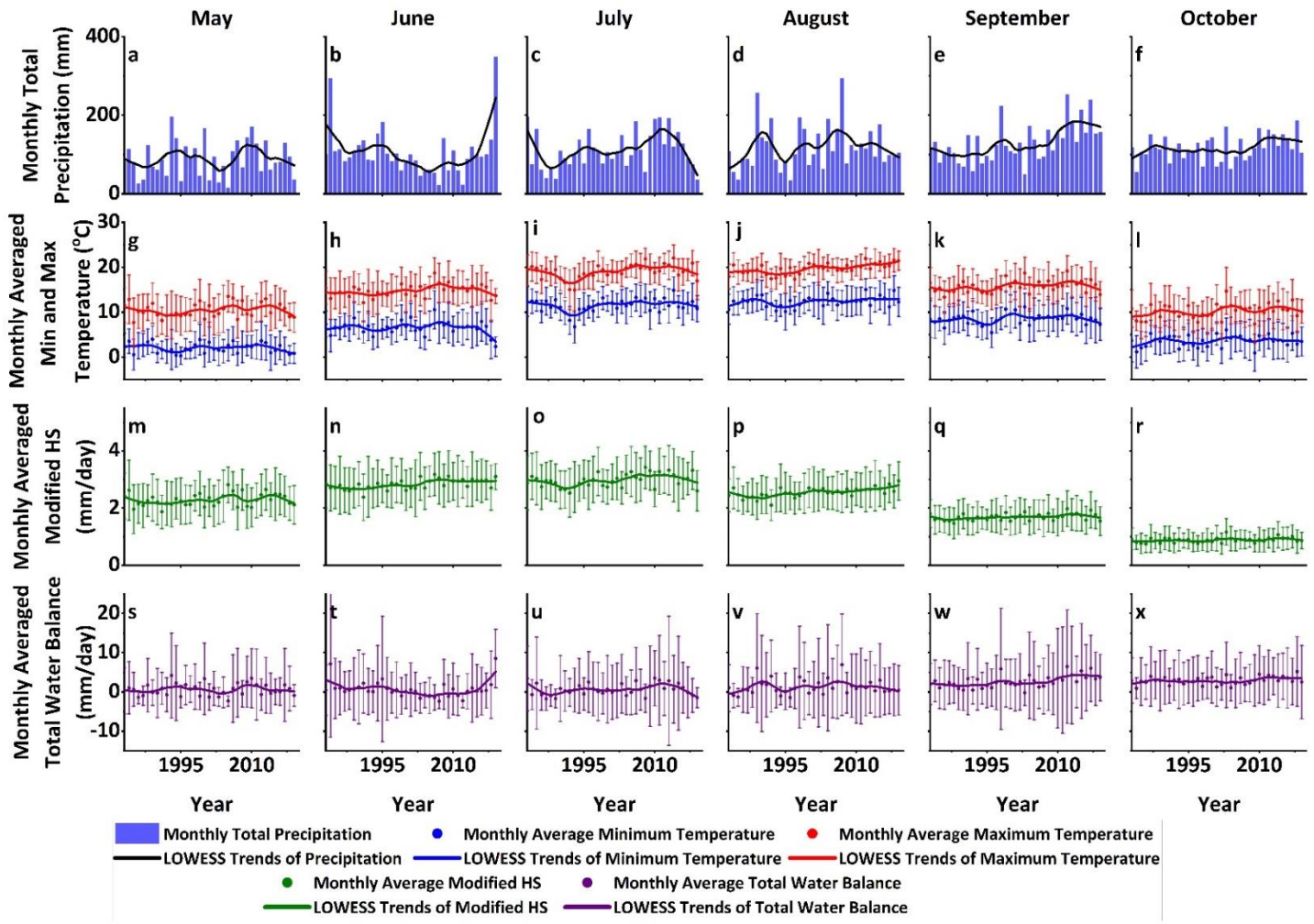

Figure 3-5: LOWESS trend analysis for Cow Head with trends of monthly total precipitation, monthly averaged min and max temperatures, monthly averaged modified HS, and monthly averaged total water balance (standard deviations are given for temperatures, PET and total water balance, No of Years = 37).

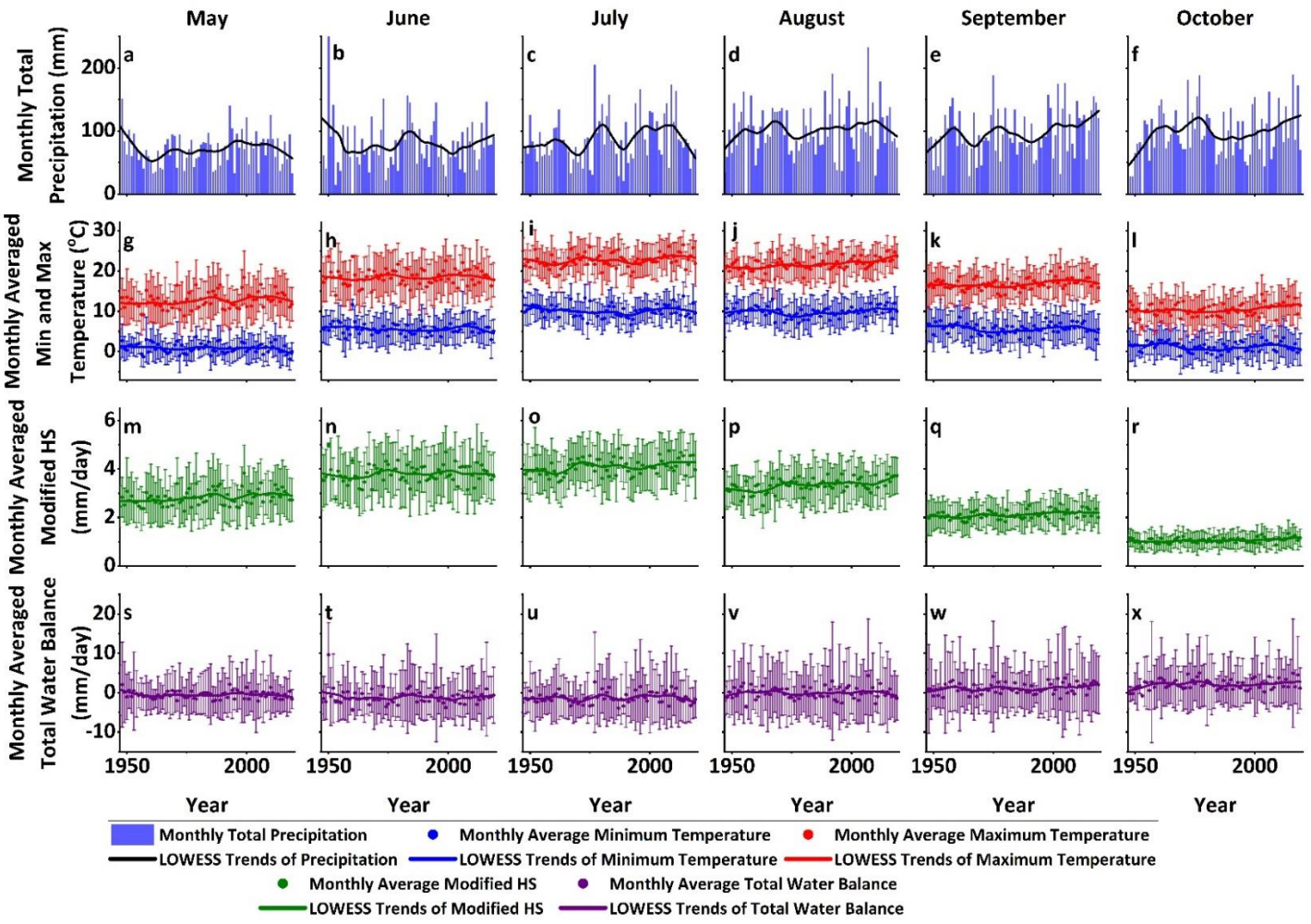

Figure 3-6: LOWESS trend analysis for Deer Lake with trends of monthly total precipitation, monthly averaged min and max temperatures, monthly averaged modified HS, and monthly averaged total water balance (standard deviations are given for temperatures, PET and total water balance, No of Years = 73).

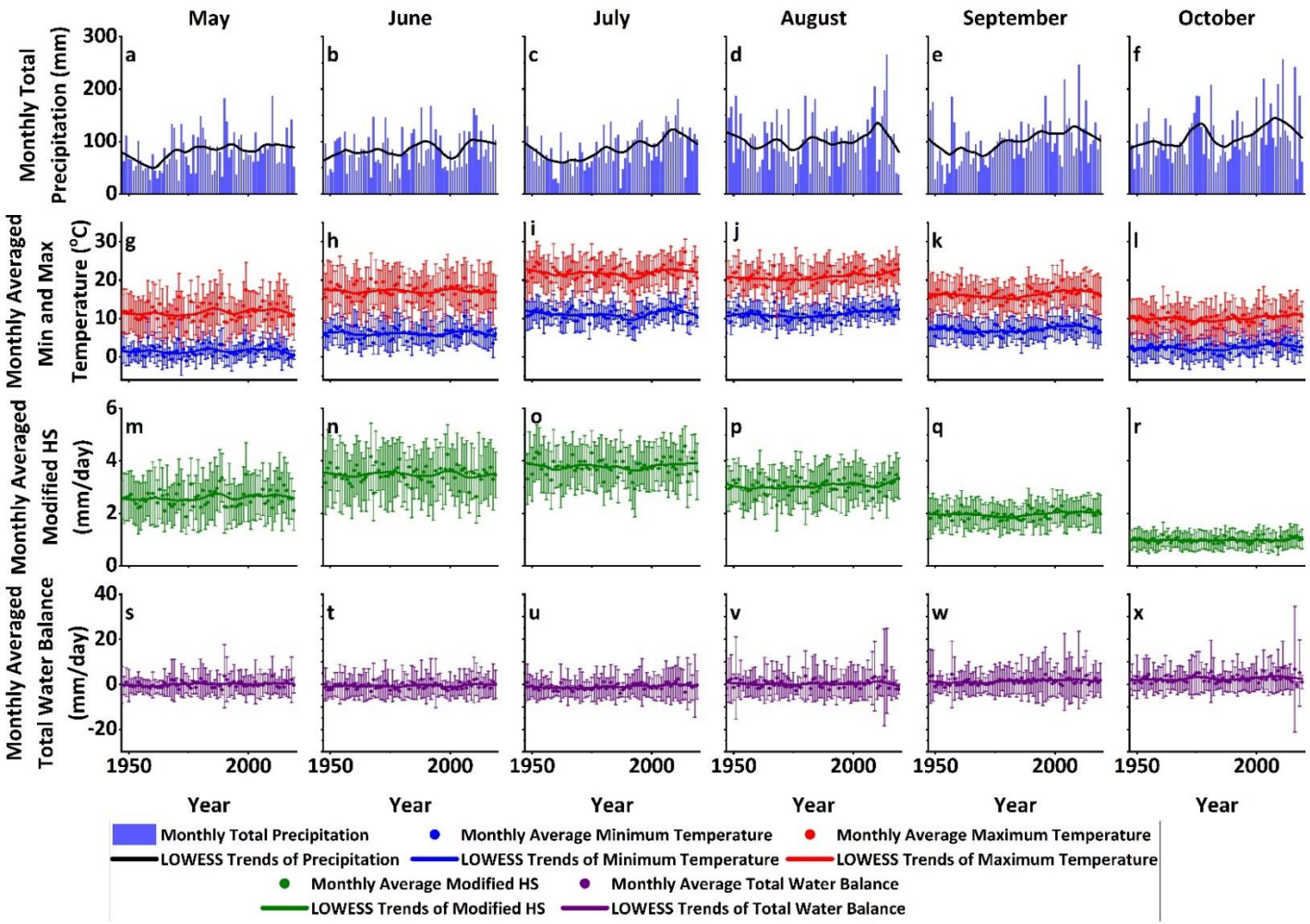

Figure 3-7: LOWESS trend analysis for Gander with trends of monthly total precipitation, monthly averaged min and max temperatures, monthly averaged modified HS, and monthly averaged total water balance (standard deviations are given for temperatures, PET and total water balance, No of Years = 73).

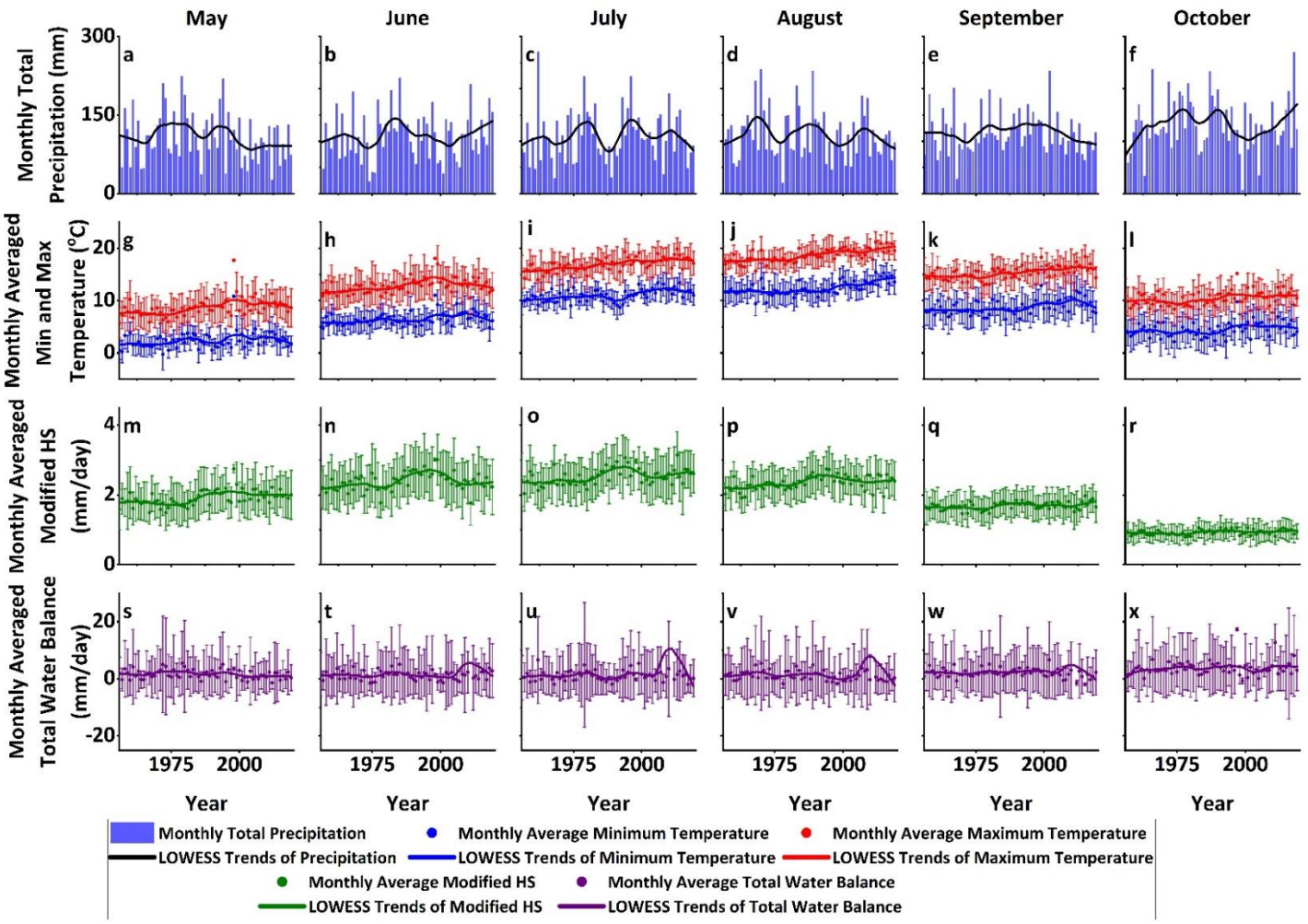

Figure 3-8: LOWESS trend analysis for Port Aux Basque with trends of monthly total precipitation, monthly averaged min and max temperatures, monthly averaged modified HS, and monthly averaged total water balance (standard deviations are given for temperatures, PET and total water balance, No of Years = 64).

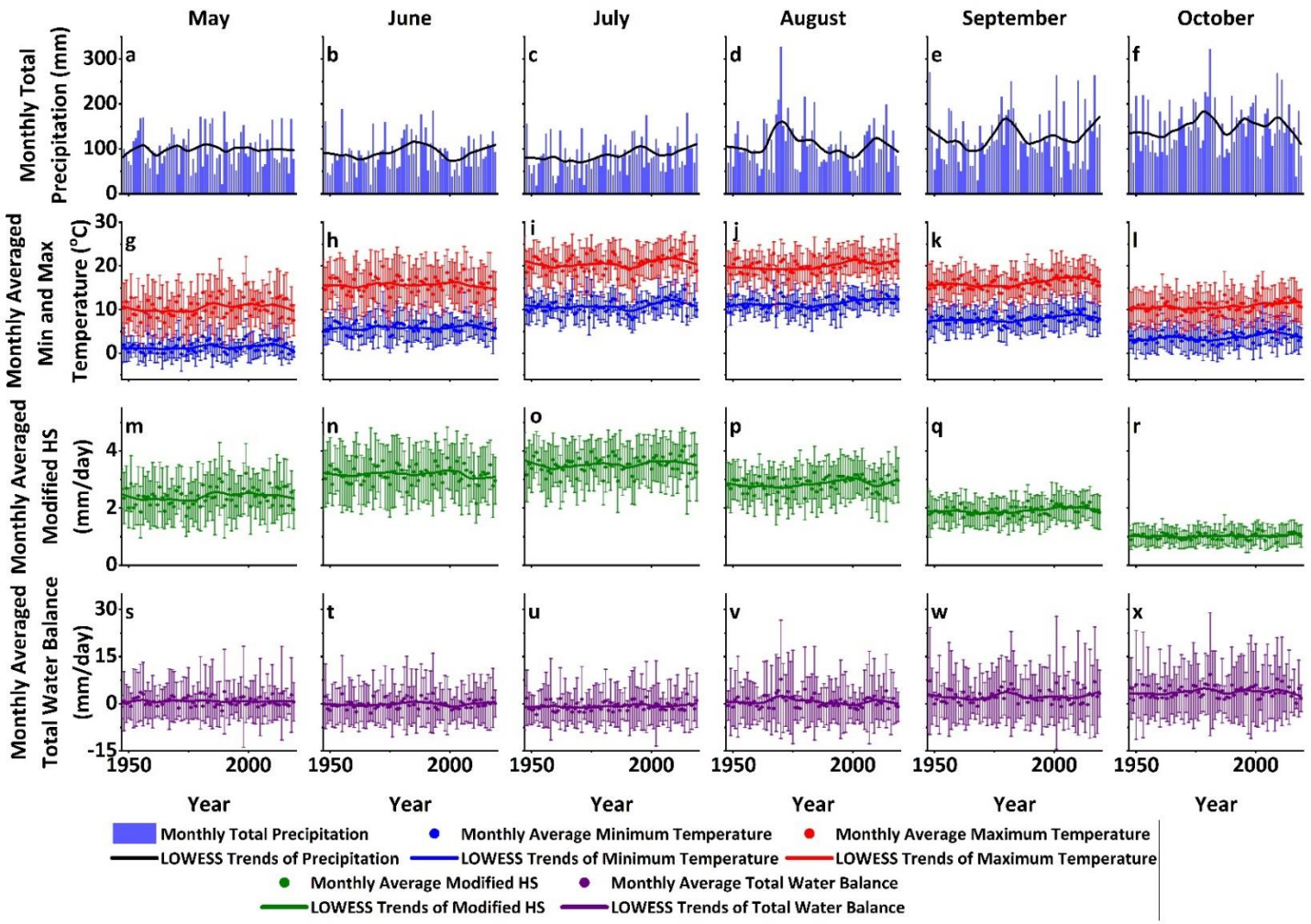

Figure 3-9: LOWESS trend analysis for St John's with trends of monthly total precipitation, monthly averaged min and max temperatures, monthly averaged modified HS, and monthly averaged total water balance (standard deviations are given for temperatures, PET and total water balance, No of Years = 73).

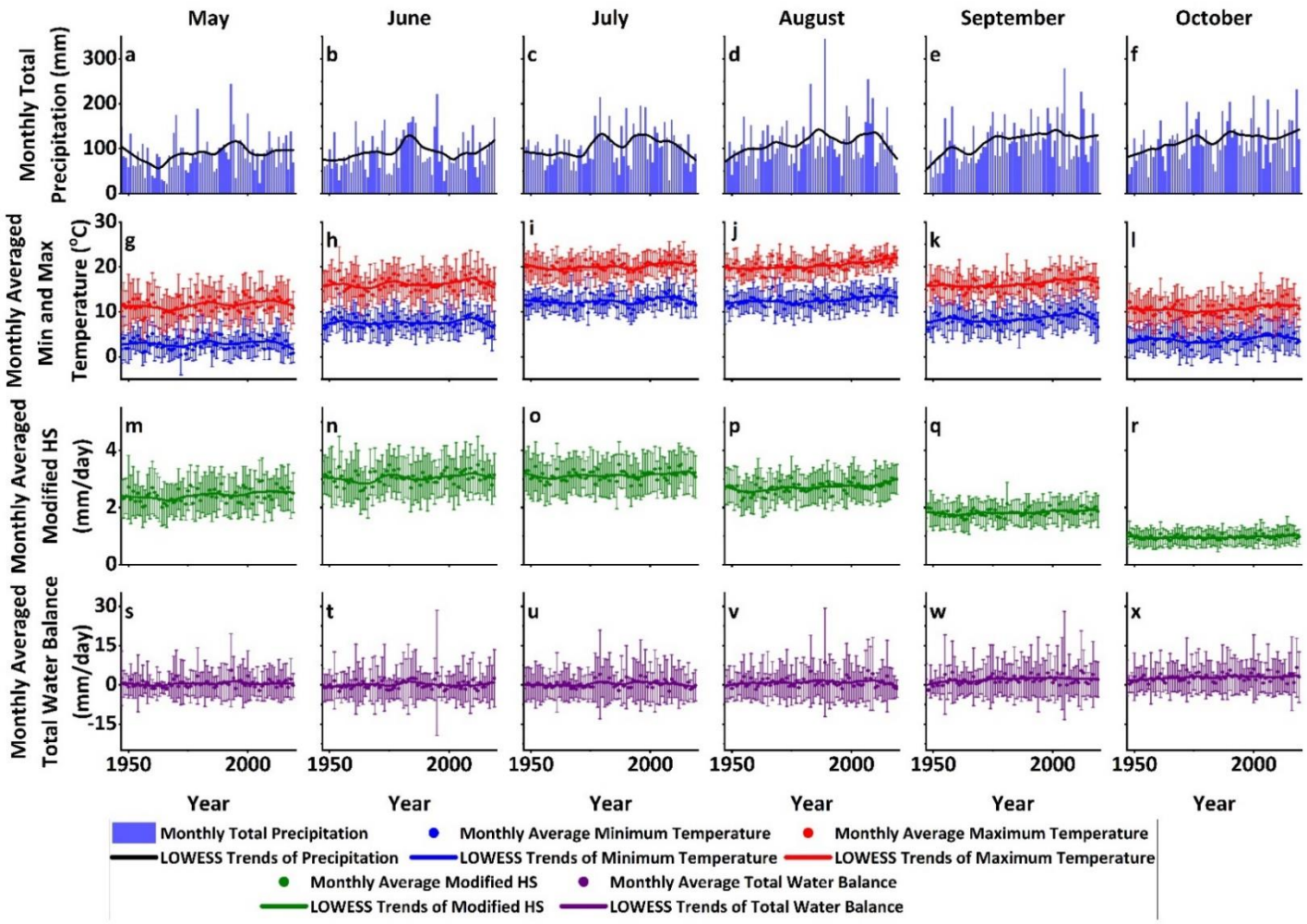

Figure 3-10: LOWESS trend analysis for Stephenville with trends of monthly total precipitation, monthly averaged min and max temperatures, monthly averaged modified HS, and monthly averaged total water balance (standard deviations are given for temperatures, PET and total water balance, No of Years = 73).

3.4.2 ITA trend analysis

ITA analysis results are presented in both graphically (Figures 3-11 to 3-18) and statistically (Table 3-3), where the D values for each parameter were calculated by using the respective plots. Controversial to the LOWESS analysis, ITA showed negative or decreasing PPT trends for *Port Aux Basque* and *St John's* (Figures 3-16 and 3-17). In contrast, the rest of the locations indicated increasing trends for May, August and October. The month of September had positive PPT trends for all location except for *St John's*, in which there was a decreasing trend (Figure 3-17-e). PPT trends for *Cormack* in July had the only negative trend compared to other locations (Figure 3-11-c). Whereas *Cow Head*, *Deer Lake* and *Port Aux Basque* showed negative trends for June (Figures 3-13-b, 3-14-b, and 3-16-b) while the remaining location had positive trends.

All locations had increasing trends for max temperature for all months except for June, where *Gander* and *St John's* had reducing trends (Figures 3-15-h, and 3-17-h). July, September and October months had positive trends for all locations in min temperature except for *Deer Lake*, which had negative trends for the three months mentioned above (Figure 3-14-o, q, and r). In addition to *Deer Lake*, *Cow Head* also showed decreasing trends in min temperature for May and June (Figures 3-13-m, and n). Furthermore, *Gander* also had reducing trends in June (Figure 3-15-n).

As shown by ITA analysis, modified HS mostly resembled the trend patterns of max temperature, which was confirmed by LOWESS analysis plots. *Cormack*, *Gander* and *St John's* had negative HS trends for all other months except June. The remaining locations had positive PET trends calculated with modified HS for all other months. ITA agreed with the LOWESS trend indications of the total water balance for September and October. *Stephenville* and *Deer Lake* were the only stations to have positive trends of total water balance for May.

Only *Cormack, Deer Lake* and *Port Aux Basque* had positive trends in June for total water balance. ITA indicated positive trends for *Cow Head, Port Aux Basque,* and *Stephenville* for July. Total water balance trends for August were negative only at *Cormack, Deer Lake* and *St John's*. It was noted that when considering both graphical and statistical results, trend identification appears to be more evident with the ITA analysis than in the LOWESS analysis.

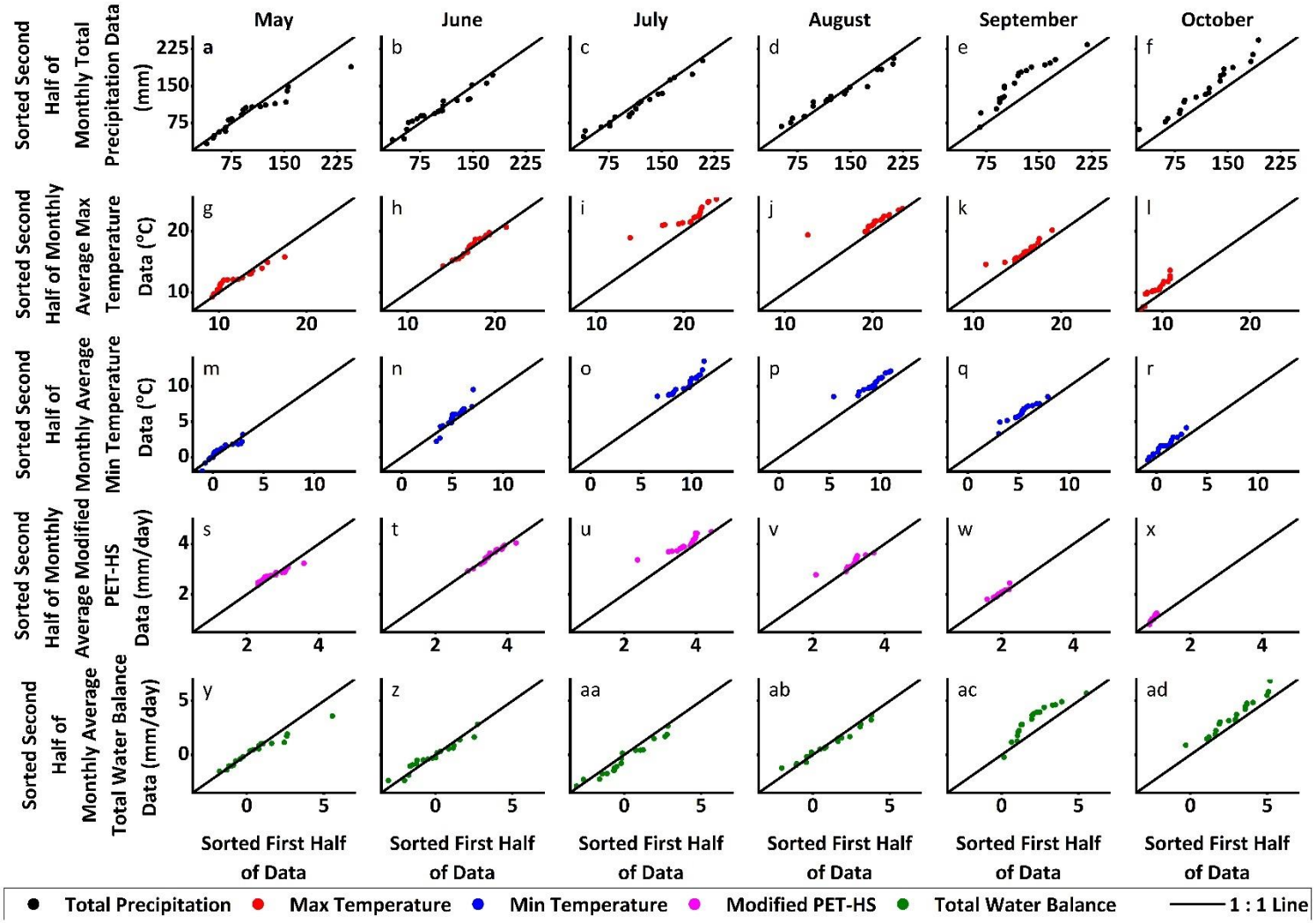

Figure 3-11: ITA analysis of Cormack, for total monthly precipitation, monthly averaged maximum temperature, monthly averaged minimum temperature, monthly averaged modified HS, and monthly averaged total water balance.

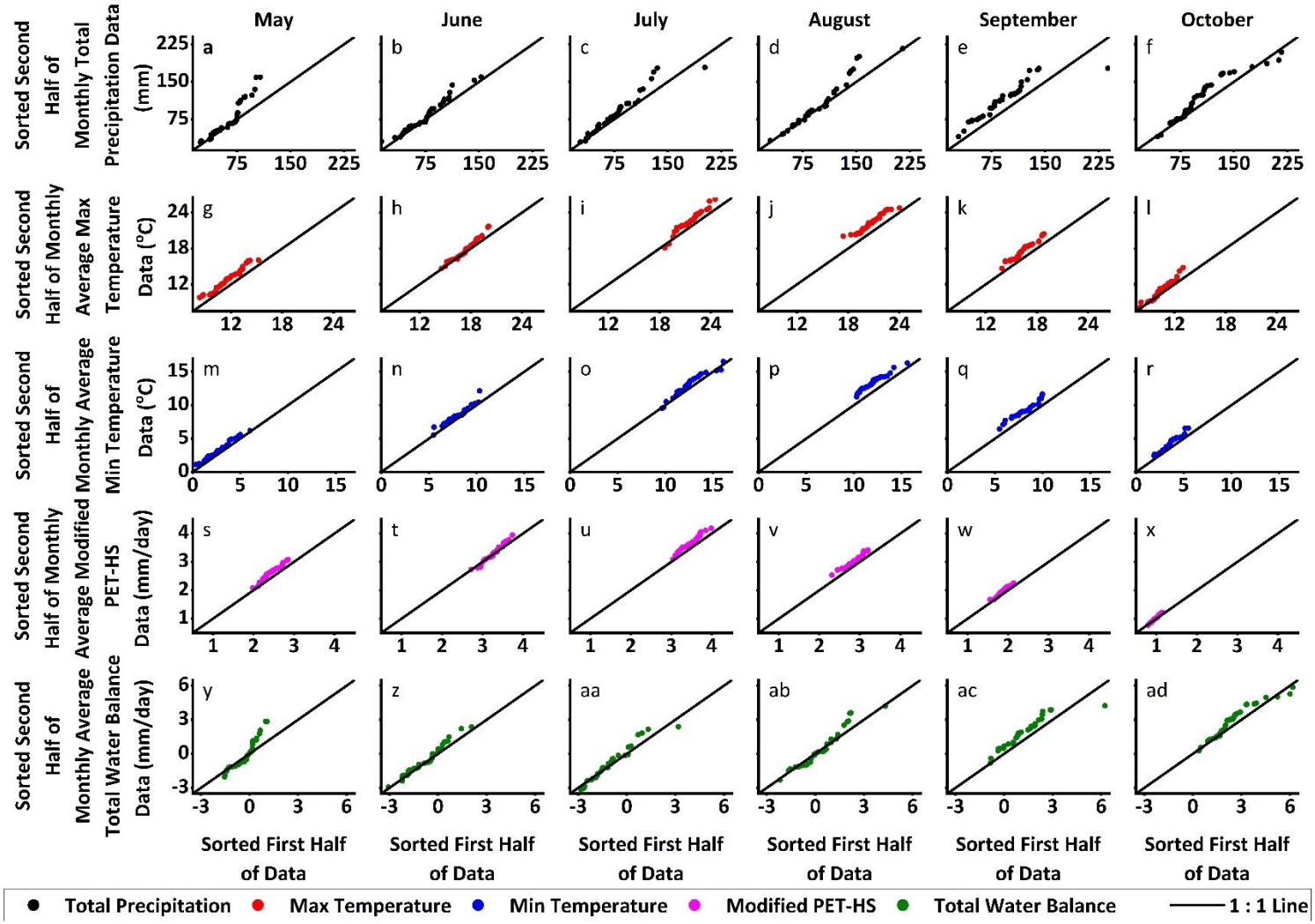

Figure 3-12: ITA analysis of Corner Brook, for total monthly precipitation, monthly averaged maximum temperature, monthly averaged minimum temperature, monthly averaged modified HS, and monthly averaged total water balance.

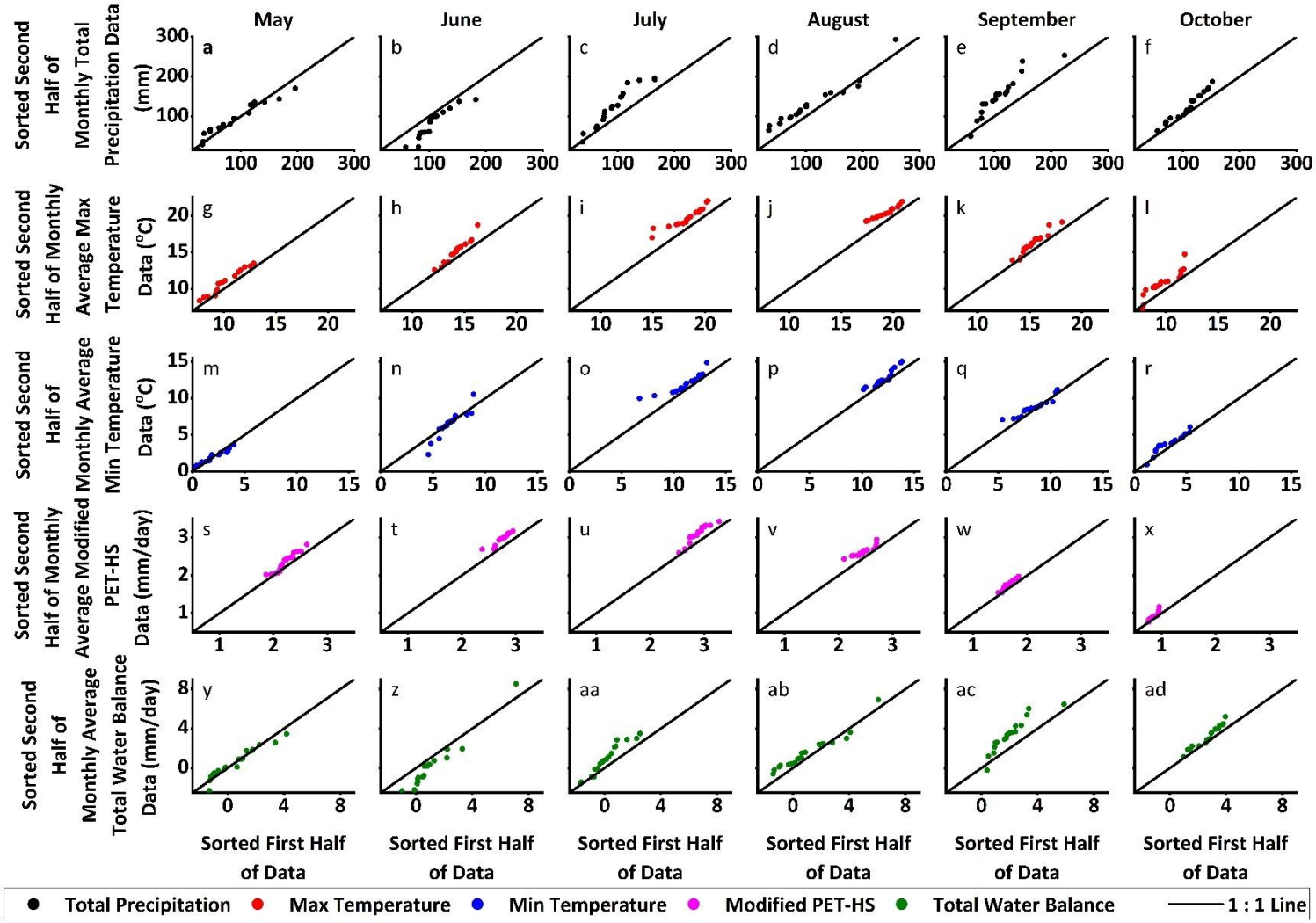

Figure 3-13: ITA analysis of Cow Head, for total monthly precipitation, monthly averaged maximum temperature, monthly averaged minimum temperature, monthly averaged modified HS, and monthly averaged total water balance.

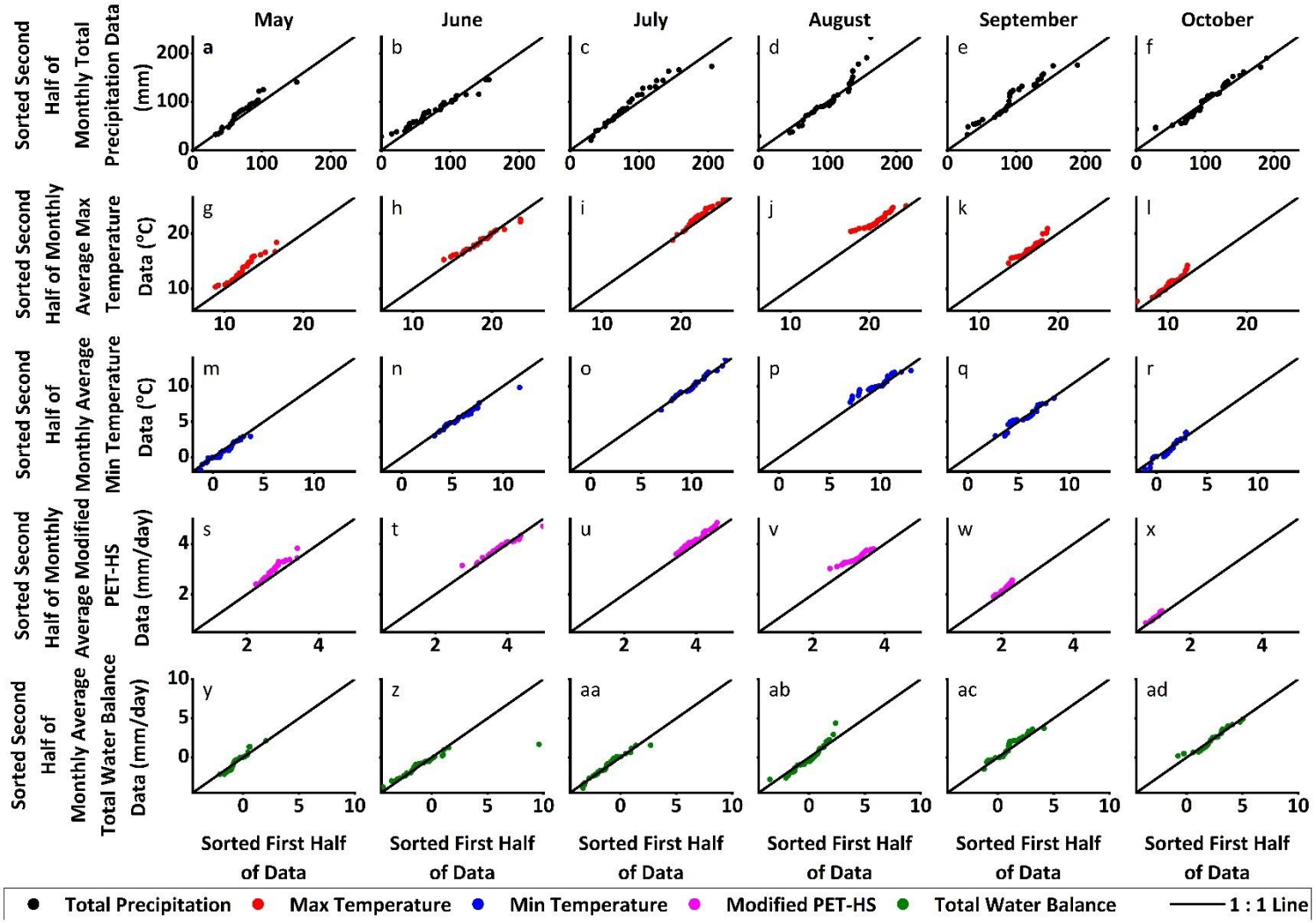

Figure 3-14: ITA analysis of Deer Lake, for total monthly precipitation, monthly averaged maximum temperature, monthly averaged minimum temperature, monthly averaged modified HS, and monthly averaged total water balance.

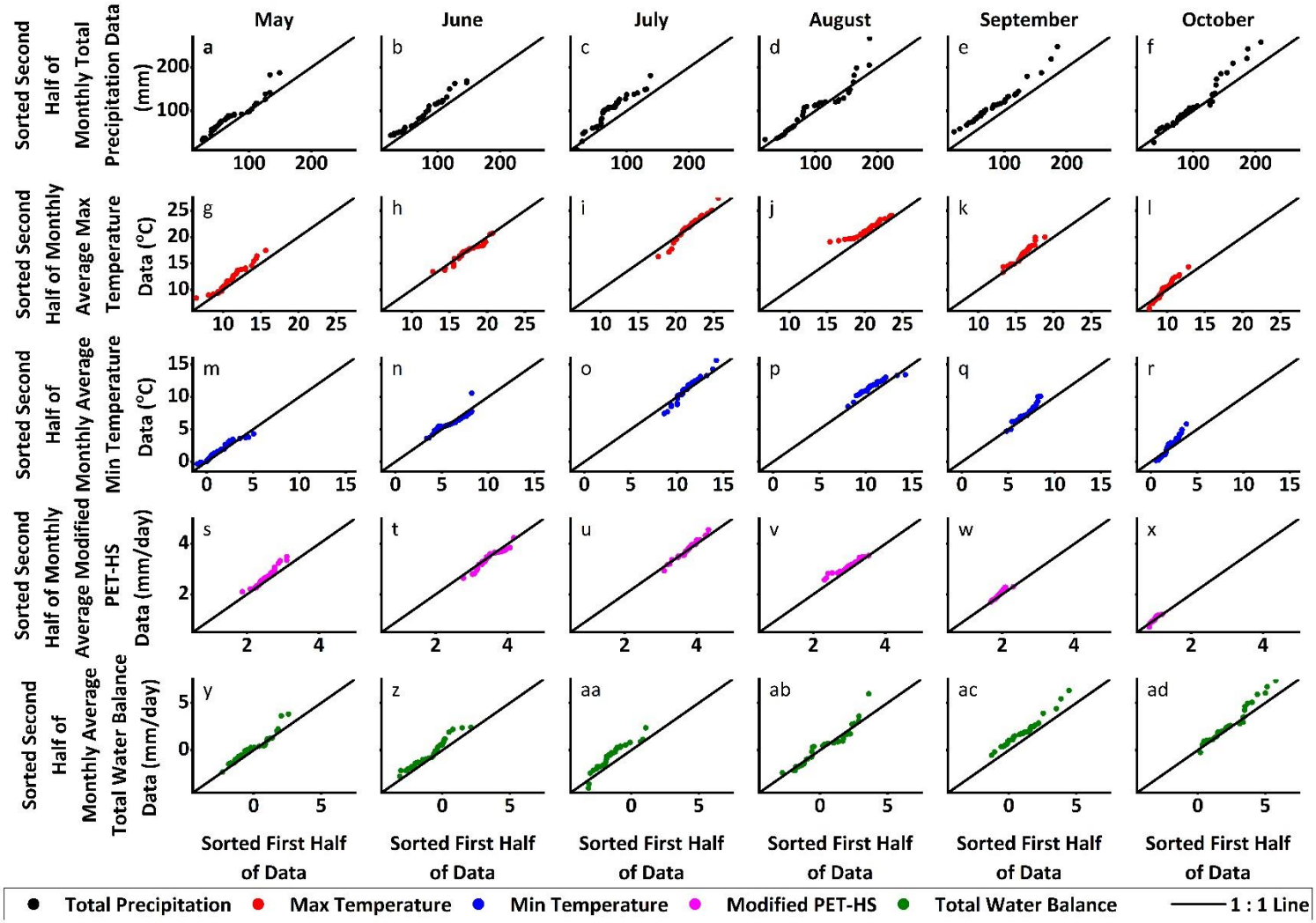

Figure 3-15: ITA analysis of Gander, for total monthly precipitation, monthly averaged maximum temperature, monthly averaged minimum temperature, monthly averaged modified HS, and monthly averaged total water balance.

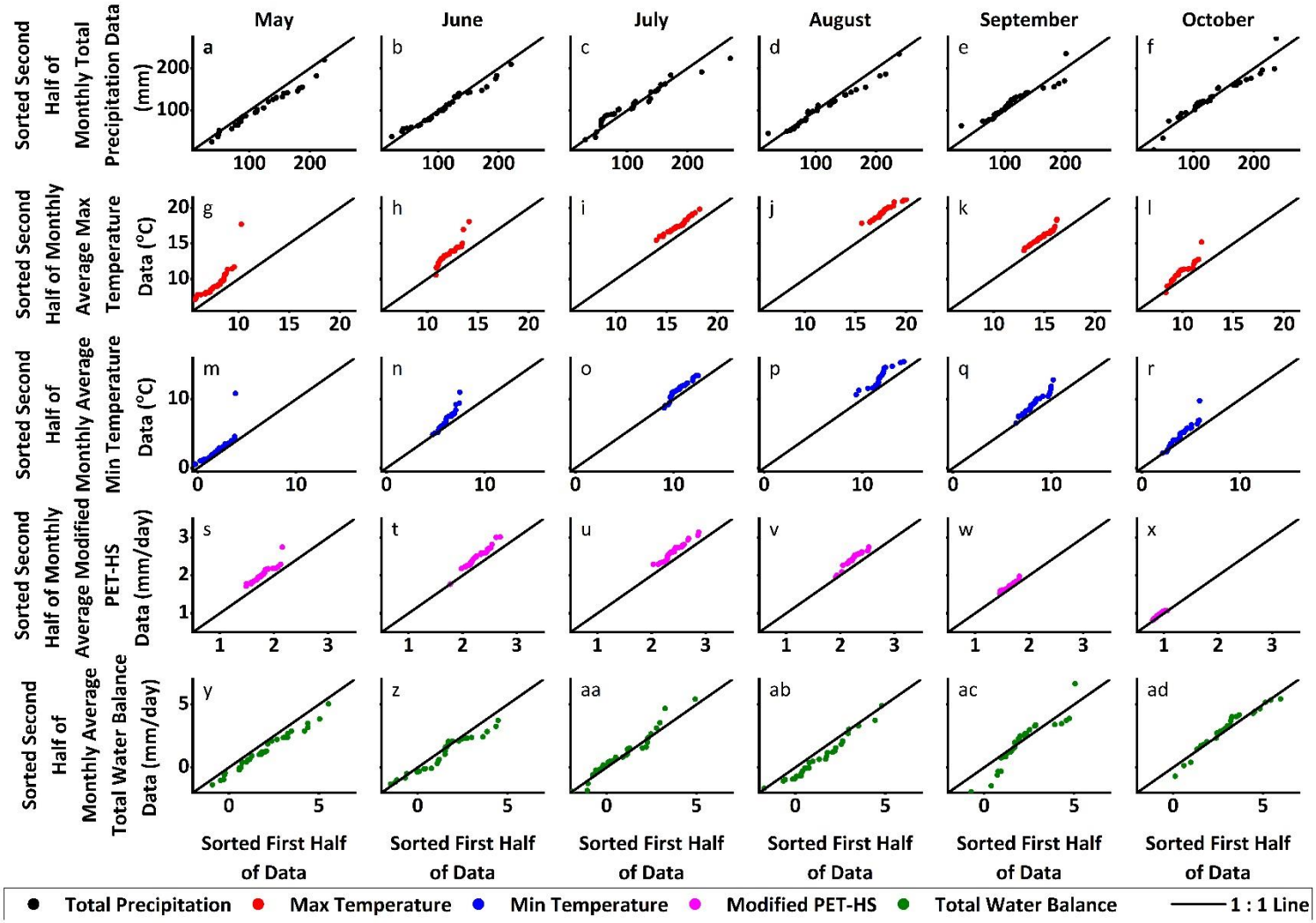

Figure 3-16: ITA analysis of Port Aux Basque, for total monthly precipitation, monthly averaged maximum temperature, monthly averaged minimum temperature, monthly averaged modified HS, and monthly averaged total water balance.

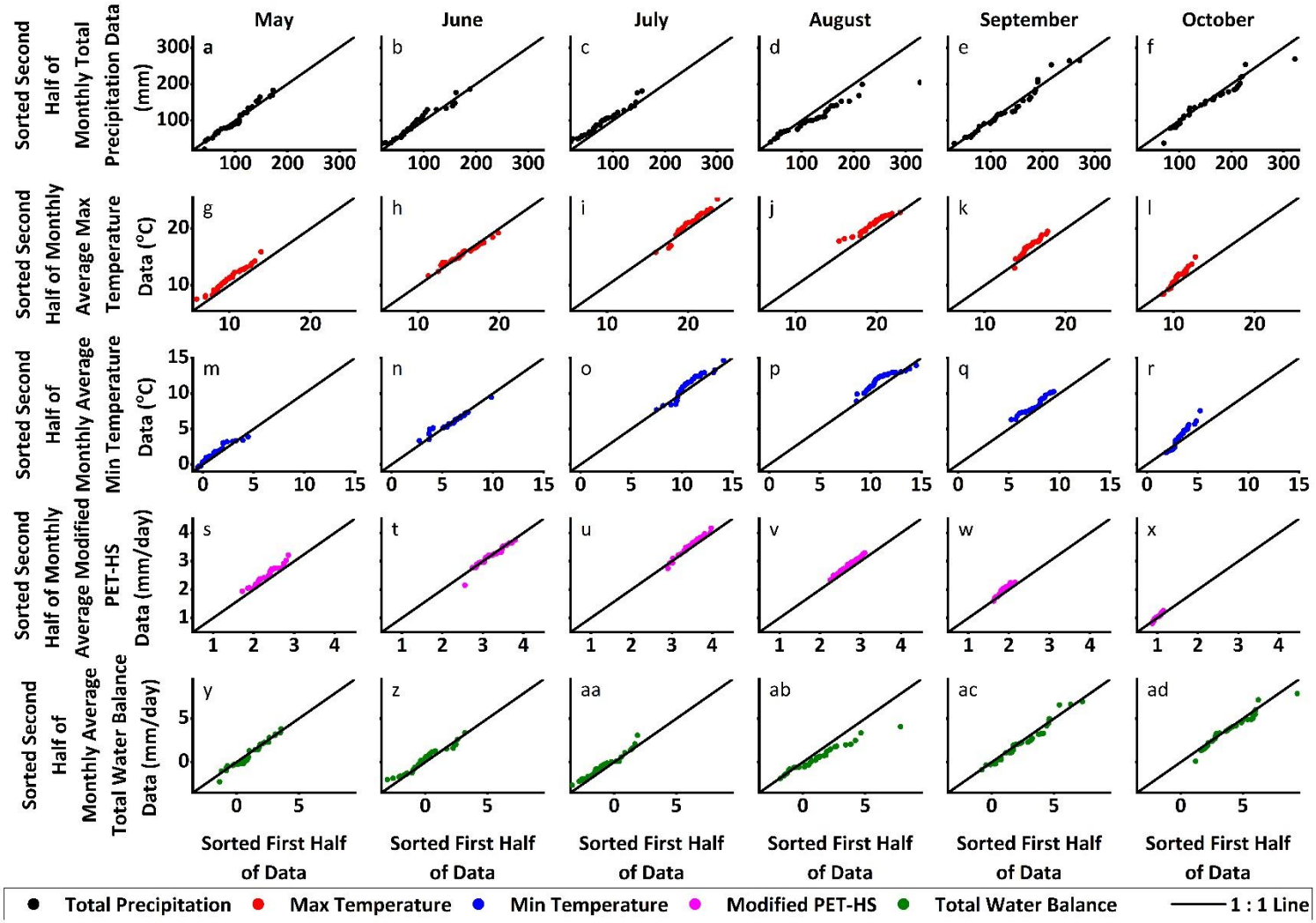

Figure 3-17: ITA analysis of St John's, for total monthly precipitation, monthly averaged maximum temperature, monthly averaged minimum temperature, monthly averaged modified HS, and monthly averaged total water balance.

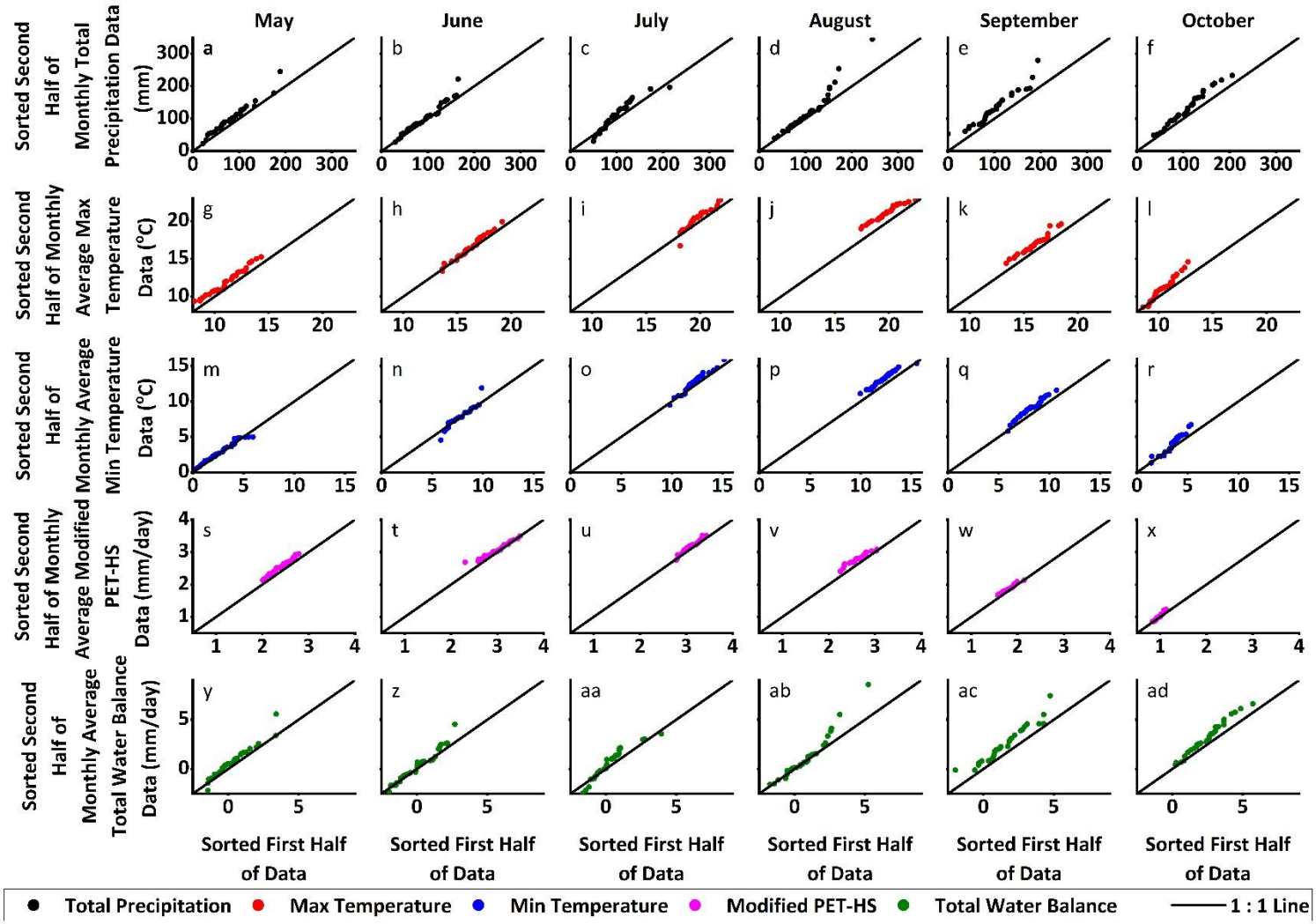

Figure 3-18: ITA analysis of Stephenville, for total monthly precipitation, monthly averaged maximum temperature, monthly averaged minimum temperature, monthly averaged modified HS, and monthly averaged total water balance.

Table 3-3: Calculated D value for ITA analysis

Month	Study Location	Total Monthly PPT		Monthly Average Max Temperature		Monthly Average Min Temperature		Monthly Average Modified HS		Monthly Average Total Water Balance	
		ITA D	**Trend**	**ITA D**	**Trend**	**ITA D**	**Trend**	**ITA D**	**Trend**	**ITA D**	**Trend**
May	*Cormack*	-0.6863	Yes (-)	0.1605	Yes (+)	0.7664	Yes (+)	0.0996	Yes (+)	-4.1655	Yes (-)
	Corner Brook	1.9755	Yes (+)	0.9931	Yes (+)	1.6745	Yes (+)	0.7227	Yes (+)	-7.85	Yes (-)
	Cow Head	0.297	Yes (+)	0.6768	Yes (+)	-0.1901	Yes (-)	0.5484	Yes (+)	-0.5859	Yes (-)
	Deer Lake	0.9195	Yes (+)	0.8706	Yes (+)	-2.5225	Yes (-)	0.7602	Yes (+)	0.0893	Yes (+)
	Gander	1.9187	Yes (+)	0.8304	Yes (+)	2.0717	Yes (+)	0.5803	Yes (+)	-20.1432	Yes (-)
	Port Aux Basque	-1.1631	Yes (-)	2.0688	Yes (+)	3.6603	Yes (+)	1.3701	Yes (+)	-3.2195	Yes (-)
	St John's	-0.0568	Yes (-)	1.1372	Yes (+)	2.8885	Yes (+)	0.7655	Yes (+)	-2.0648	Yes (-)
	Stephenville	2.0615	Yes (+)	0.7395	Yes (+)	0.4968	Yes (+)	0.6226	Yes (+)	17.412	Yes (+)
June	*Cormack*	0.041	Yes (+)	0.1175	Yes (+)	5.1908	Yes (+)	-0.0113	Yes (-)	0.2783	Yes (+)
	Corner Brook	0.8626	Yes (+)	0.2199	Yes (+)	0.6141	Yes (+)	0.0993	Yes (+)	-2.4405	Yes (-)
	Cow Head	-2.3741	Yes (-)	0.9289	Yes (+)	-0.7296	Yes (-)	0.9726	Yes (+)	-14.4829	Yes (-)
	Deer Lake	-0.3311	Yes (-)	0.0414	Yes (+)	-0.4812	Yes (-)	0.1152	Yes (+)	1.345	Yes (+)
	Gander	1.931	Yes (+)	-0.1352	Yes (-)	-0.0313	Yes (-)	-0.1362	Yes (-)	-5.9379	Yes (-)
	Port Aux Basque	-0.2539	Yes (-)	1.8134	Yes (+)	4.1526	Yes (+)	1.1834	Yes (+)	3.77	Yes (+)
	St John's	0.7486	Yes (+)	-0.005	Yes (-)	0.1601	Yes (+)	-0.0588	Yes (-)	-10.7587	Yes (-)
	Stephenville	0.9671	Yes (+)	0.1747	Yes (+)	0.0617	Yes (+)	0.227	Yes (+)	-33.5053	Yes (-)
July	*Cormack*	-0.4271	Yes (-)	1.4292	Yes (+)	11.8551	Yes (+)	1.0785	Yes (+)	-7.4125	Yes (-)
	Corner Brook	1.2076	Yes (+)	0.457	Yes (+)	0.4433	Yes (+)	0.5165	Yes (+)	-1.2543	Yes (-)
	Cow Head	3.4076	Yes (+)	1.4731	Yes (+)	4.4705	Yes (+)	0.9374	Yes (+)	12.0818	Yes (+)
	Deer Lake	0.7335	Yes (+)	0.3119	Yes (+)	-0.016	Yes (-)	0.4267	Yes (+)	-0.2296	Yes (-)

	Gander	3.4488	Yes (+)	0.0544	Yes (+)	0.052	Yes (+)	0.0671	Yes (+)	-5.6542	Yes (-)
	Port Aux Basque	0.2837	Yes (+)	1.8033	Yes (+)	4.1298	Yes (+)	1.2344	Yes (+)	12.064	Yes (+)
	St John's	1.894	Yes (+)	0.3176	Yes (+)	0.469	Yes (+)	0.2463	Yes (+)	-4.2058	Yes (-)
	Stephenville	0.98	Yes (+)	0.2959	Yes (+)	0.3491	Yes (+)	0.2455	Yes (+)	16.3017	Yes (+)
August	*Cormack*	0.0767	Yes (+)	1.037	Yes (+)	14.2573	Yes (+)	0.4823	Yes (+)	-1.6107	Yes (-)
	Corner Brook	0.7299	Yes (+)	0.7716	Yes (+)	1.1231	Yes (+)	0.6189	Yes (+)	1.9009	Yes (+)
	Cow Head	2.3383	Yes (+)	1.218	Yes (+)	3.0153	Yes (+)	0.7762	Yes (+)	7.8237	Yes (+)
	Deer Lake	0.5061	Yes (+)	0.6396	Yes (+)	0.4814	Yes (+)	0.7271	Yes (+)	-22.5751	Yes (-)
	Gander	0.788	Yes (+)	0.5543	Yes (+)	0.8089	Yes (+)	0.4421	Yes (+)	5.231	Yes (+)
	Port Aux Basque	-0.5246	Yes (-)	2.1466	Yes (+)	6.1805	Yes (+)	1.126	Yes (+)	4.9866	Yes (+)
	St John's	-1.4149	Yes (-)	0.6481	Yes (+)	0.8126	Yes (+)	0.5368	Yes (+)	-6.6763	Yes (-)
	Stephenville	1.4382	Yes (+)	0.6491	Yes (+)	0.7402	Yes (+)	0.5913	Yes (+)	4.2521	Yes (+)
September	*Cormack*	2.8743	Yes (+)	0.7189	Yes (+)	11.9194	Yes (+)	0.2689	Yes (+)	17.7408	Yes (+)
	Corner Brook	2.3421	Yes (+)	0.7444	Yes (+)	1.3808	Yes (+)	0.4562	Yes (+)	5.2418	Yes (+)
	Cow Head	4.7419	Yes (+)	0.8586	Yes (+)	1.7451	Yes (+)	0.4294	Yes (+)	20.5984	Yes (+)
	Deer Lake	1.2484	Yes (+)	0.4984	Yes (+)	-0.0395	Yes (-)	0.5724	Yes (+)	2.6464	Yes (+)
	Gander	3.303	Yes (+)	0.5035	Yes (+)	0.767	Yes (+)	0.3954	Yes (+)	9.2241	Yes (+)
	Port Aux Basque	0.3491	Yes (+)	1.5435	Yes (+)	5.2789	Yes (+)	0.4323	Yes (+)	3.8083	Yes (+)
	St John's	-0.1884	Yes (-)	0.7667	Yes (+)	0.9094	Yes (+)	0.652	Yes (+)	-0.8396	Yes (-)
	Stephenville	3.0655	Yes (+)	0.5969	Yes (+)	1.0346	Yes (+)	0.3475	Yes (+)	6.2699	Yes (+)
October	*Cormack*	2.1607	Yes (+)	0.9941	Yes (+)	9.8486	Yes (+)	0.2595	Yes (+)	12.4377	Yes (+)
	Corner Brook	1.1144	Yes (+)	0.5385	Yes (+)	1.8125	Yes (+)	0.2188	Yes (+)	1.4613	Yes (+)
	Cow Head	1.8485	Yes (+)	1.0865	Yes (+)	2.3335	Yes (+)	0.2817	Yes (+)	7.3504	Yes (+)
	Deer Lake	0.093	Yes (+)	0.5963	Yes (+)	-1.1949	Yes (-)	0.543	Yes (+)	-0.123	Yes (-)
	Gander	1.1007	Yes (+)	0.462	Yes (+)	2.2758	Yes (+)	0.1674	Yes (+)	1.476	Yes (+)
	Port Aux Basque	-0.0552	Yes (-)	1.2836	Yes (+)	4.3668	Yes (+)	0.2635	Yes (+)	3.4434	Yes (+)

St John's	-0.442	Yes (-)	0.6385	Yes (+)	2.0161	Yes (+)	0.2476	Yes (+)	-0.6181	Yes (-)
Stephenville	2.038	Yes (+)	0.6064	Yes (+)	1.4899	Yes (+)	0.3128	Yes (+)	2.7003	Yes (+)

Table 3-4: Calculated Z values for MK test and the Sen's slope values for each location and parameter.

Month	Study Location	Total Monthly PPT				Max Temperature				Min Temperature				Modified HS				Total Water Balance			
		MK Z	Trend at 95% CL	Trend at 90% CL	Sen's Slope	MK Z	Trend at 95% CL	Trend at 90% CL	Sen's Slope	MK Z	Trend at 95% CL	Trend at 90% CL	Sen's Slope	MK Z	Trend at 95% CL	Trend at 90% CL	Sen's Slope	MK Z	Trend at 95% CL	Trend at 90% CL	Sen's Slope
May	*Cormack*	-0.0484	No	No	-0.0364	-0.3872	No	No	-0.0081	-0.2662	No	No	-0.0047	0.0484	No	No	0.0003	0.0726	No	No	0.0028
	Corner Brook	0.6334	No	No	0.1078	2.2241	Yes (+)	Yes (+)	0.0236	1.6954	No	Yes (+)	0.0116	2.2716	Yes (+)	Yes (+)	0.0036	0.0238	No	No	0.0003
	Cow Head	0.6147	No	No	0.4333	0.4447	No	No	0.0183	-0.6671	No	No	-0.0094	1.0332	No	No	0.0042	0.4054	No	No	0.0077
	Deer Lake	0.5667	No	No	0.0797	2.0430	Yes (+)	Yes (+)	0.0206	-1.1144	No	No	-0.0070	2.5955	Yes (+)	Yes (+)	0.0045	-0.7477	No	No	-0.0042
	Gander	2.1907	Yes (+)	Yes (+)	0.4165	1.2334	No	No	0.0131	0.8810	No	No	0.0068	1.2144	No	No	0.0021	1.6335	No	No	0.0103
	Port Aux Basque	-1.3267	No	No	-0.4059	4.4438	Yes (+)	Yes (+)	0.0359	2.3696	Yes (+)	Yes (+)	0.0173	3.9686	Yes (+)	Yes (+)	0.0055	-1.6280	No	No	-0.0190
	St John's	0.0381	No	No	0.0098	1.5192	No	No	0.0187	1.5288	No	No	0.0092	1.4906	No	No	0.0022	-0.1953	No	No	-0.0019
	Stephenville	1.8621	No	Yes (+)	0.3754	1.9764	Yes (+)	Yes (+)	0.0192	0.5048	No	No	0.0039	2.7669	Yes (+)	Yes (+)	0.0037	1.3668	No	No	0.0084
June	*Cormack*	-0.3145	No	No	-0.2333	0.0726	No	No	0.0027	0.5323	No	No	0.0111	0.1936	No	No	0.0012	-0.1936	No	No	-0.0069
	Corner Brook	1.1239	No	No	0.1773	1.8050	No	Yes (+)	0.0153	2.6289	Yes (+)	Yes (+)	0.0166	1.0620	No	No	0.0016	0.7667	No	No	0.0051
	Cow Head	-1.1117	No	No	-0.6606	1.9097	No	Yes (+)	0.0368	-0.1570	No	No	-0.0026	3.3613	Yes (+)	Yes (+)	0.0085	-1.3733	No	No	-0.0260
	Deer Lake	0.9572	No	No	0.2029	0.8763	No	No	0.0080	-0.7572	No	No	-0.0050	1.2715	No	No	0.0023	0.4810	No	No	0.0032
	Gander	1.5526	No	No	0.2879	-0.0095	No	No	-0.0001	-0.1381	No	No	-0.0010	0.0333	No	No	0.0001	1.2430	No	No	0.0096
	Port Aux Basque	0.6141	No	No	0.1895	3.9457	Yes (+)	Yes (+)	0.0348	3.5399	Yes (+)	Yes (+)	0.0238	2.4507	Yes (+)	Yes (+)	0.0038	0.2955	No	No	0.0041
	St John's	1.0382	No	No	0.2000	-0.0429	No	No	-0.0004	0.5382	No	No	0.0034	-0.2715	No	No	-0.0005	0.9477	No	No	0.0073
	Stephenville	1.1859	No	No	0.2633	1.7573	No	Yes (+)	0.0148	0.6667	No	No	0.0053	1.8906	No	Yes (+)	0.0025	0.6715	No	No	0.0058

July	*Cormack*	-0.7138	No	No	-0.5471	2.5645	Yes (+)	Yes (+)	0.0618	1.2581	No	No	0.0311	2.3226	Yes (+)	Yes (+)	0.0109	-1.1613	No	No	-0.0260
	Corner Brook	0.9477	No	No	0.1717	2.9861	Yes (+)	Yes (+)	0.0266	2.5480	Yes (+)	Yes (+)	0.0183	2.7479	Yes (+)	Yes (+)	0.0038	0.2334	No	No	0.0016
	Cow Head	1.4518	No	No	1.1308	2.1584	Yes (+)	Yes (+)	0.0491	1.0857	No	No	0.0227	2.0272	Yes (+)	Yes (+)	0.0082	1.0332	No	No	0.0255
	Deer Lake	1.4335	No	No	0.2467	2.3288	Yes (+)	Yes (+)	0.0209	-0.9906	No	No	-0.0085	2.6907	Yes (+)	Yes (+)	0.0051	0.5858	No	No	0.0041
	Gander	3.5052	Yes (+)	Yes (+)	0.6892	0.6048	No	No	0.0072	0.4572	No	No	0.0033	0.2715	No	No	0.0004	3.1574	Yes (+)	Yes (+)	0.0234
	Port Aux Basque	0.7184	No	No	0.2523	5.4404	Yes (+)	Yes (+)	0.0437	4.2931	Yes (+)	Yes (+)	0.0337	3.6094	Yes (+)	Yes (+)	0.0056	0.6894	No	No	0.0069
	St John's	1.8907	No	Yes (+)	0.4345	1.9335	No	Yes (+)	0.0213	1.8955	No	Yes (+)	0.0164	1.5573	No	No	0.0025	1.4430	No	No	0.0117
	Stephenville	1.5763	No	No	0.3194	2.5193	Yes (+)	Yes (+)	0.0160	1.5050	No	No	0.0098	2.2050	Yes (+)	Yes (+)	0.0021	1.4620	No	No	0.0088
August	*Cormack*	-0.0242	No	No	-0.0056	3.0123	Yes (+)	Yes (+)	0.0560	3.4360	Yes (+)	Yes (+)	0.0558	1.9839	Yes (+)	Yes (+)	0.0064	-0.7016	No	No	-0.0092
	Corner Brook	1.1668	No	No	0.2603	5.0435	Yes (+)	Yes (+)	0.0427	5.3674	Yes (+)	Yes (+)	0.0376	3.2336	Yes (+)	Yes (+)	0.0042	0.3000	No	No	0.0028
	Cow Head	1.0855	No	No	0.8635	3.7932	Yes (+)	Yes (+)	0.0682	1.3735	No	No	0.0253	3.7798	Yes (+)	Yes (+)	0.0095	0.5624	No	No	0.0160
	Deer Lake	0.6239	No	No	0.1250	4.2434	Yes (+)	Yes (+)	0.0335	1.1525	No	No	0.0081	3.9480	Yes (+)	Yes (+)	0.0059	-0.3000	No	No	-0.0025
	Gander	0.3762	No	No	0.1150	2.5859	Yes (+)	Yes (+)	0.0240	3.1813	Yes (+)	Yes (+)	0.0231	1.7287	No	Yes (+)	0.0026	0.0238	No	No	0.0002
	Port Aux Basque	-0.7069	No	No	-0.1837	5.9849	Yes (+)	Yes (+)	0.0500	4.7335	Yes (+)	Yes (+)	0.0365	4.0613	Yes (+)	Yes (+)	0.0052	-1.6280	No	No	-0.0189
	St John's	-0.2715	No	No	-0.0946	2.7860	Yes (+)	Yes (+)	0.0270	3.1955	Yes (+)	Yes (+)	0.0254	2.0430	Yes (+)	Yes (+)	0.0029	-0.5953	No	No	-0.0050
	Stephenville	1.3144	No	No	0.3240	4.9006	Yes (+)	Yes (+)	0.0328	3.6576	Yes (+)	Yes (+)	0.0218	4.0623	Yes (+)	Yes (+)	0.0040	0.8906	No	No	0.0071
September	*Cormack*	2.7101	Yes (+)	Yes (+)	1.6676	1.1859	No	No	0.0231	1.9842	Yes (+)	Yes (+)	0.0333	1.2339	No	No	0.0024	2.5403	Yes (+)	Yes (+)	0.0545
	Corner Brook	2.7194	Yes (+)	Yes (+)	0.5574	3.8197	Yes (+)	Yes (+)	0.0265	4.4006	Yes (+)	Yes (+)	0.0292	1.4430	No	No	0.0014	2.4717	Yes (+)	Yes (+)	0.0178
	Cow Head	3.4136	Yes (+)	Yes (+)	2.2100	1.7789	No	Yes (+)	0.0413	0.9156	No	No	0.0146	2.0795	Yes (+)	Yes (+)	0.0044	3.3613	Yes (+)	Yes (+)	0.0755
	Deer Lake	1.8811	No	Yes (+)	0.4271	2.5479	Yes (+)	Yes (+)	0.0172	-1.0620	No	No	-0.0085	3.2146	Yes (+)	Yes (+)	0.0030	1.3192	No	No	0.0103
	Gander	3.1384	Yes (+)	Yes (+)	0.7063	2.0288	Yes (+)	Yes (+)	0.0150	1.7478	No	Yes (+)	0.0108	1.7573	No	Yes (+)	0.0015	2.8526	Yes (+)	Yes (+)	0.0221
	Port Aux Basque	-0.1448	No	No	-0.0354	4.2815	Yes (+)	Yes (+)	0.0342	3.6211	Yes (+)	Yes (+)	0.0291	2.8099	Yes (+)	Yes (+)	0.0021	-0.7126	No	No	-0.0092
	St John's	0.5953	No	No	0.1979	3.6004	Yes (+)	Yes (+)	0.0257	2.9194	Yes (+)	Yes (+)	0.0177	2.8336	Yes (+)	Yes (+)	0.0024	0.4143	No	No	0.0053
	Stephenville	3.0575	Yes (+)	Yes (+)	0.7694	3.8146	Yes (+)	Yes (+)	0.0248	3.1004	Yes (+)	Yes (+)	0.0227	2.6336	Yes (+)	Yes (+)	0.0019	2.7669	Yes (+)	Yes (+)	0.0238
October	*Cormack*	1.8387	No	Yes (+)	1.4333	1.5364	No	No	0.0357	1.4401	No	No	0.0219	1.2097	No	No	0.0015	1.6936	No	Yes (+)	0.0419
	Corner Brook	2.1002	Yes (+)	Yes (+)	0.5111	2.1193	Yes (+)	Yes (+)	0.0175	3.1814	Yes (+)	Yes (+)	0.0198	1.1287	No	No	0.0006	2.0049	Yes (+)	Yes (+)	0.0162

Cow Head	**1.6613**	**No**	**Yes (+)**	**0.9618**	**1.4520**	**No**	**No**	**0.0462**	**0.8111**	**No**	**No**	**0.0174**	**1.7133**	**No**	**Yes (+)**	**0.0023**	**1.5302**	**No**	**No**	**0.0272**
Deer Lake	**1.4335**	**No**	**No**	**0.3595**	**1.9478**	**No**	**Yes (+)**	**0.0190**	**-1.0811**	**No**	**No**	**-0.0076**	**2.9955**	**Yes (+)**	**Yes (+)**	**0.0018**	**1.1477**	**No**	**No**	**0.0086**
Gander	**1.6145**	**No**	**No**	**0.4460**	**1.6954**	**No**	**Yes (+)**	**0.0128**	**1.9240**	**No**	**Yes (+)**	**0.0140**	**0.7763**	**No**	**No**	**0.0003**	**1.6240**	**No**	**No**	**0.0139**
Port Aux Basque	**0.3071**	**No**	**No**	**0.1005**	**2.9837**	**Yes (+)**	**Yes (+)**	**0.0259**	**2.5029**	**Yes (+)**	**Yes (+)**	**0.0212**	**2.2885**	**Yes (+)**	**Yes (+)**	**0.0013**	**0.6779**	**No**	**No**	**0.0083**
St John's	**0.9572**	**No**	**No**	**0.3068**	**2.4336**	**Yes (+)**	**Yes (+)**	**0.017196**	**3.0765**	**Yes (+)**	**Yes (+)**	**0.0200**	**1.4049**	**No**	**No**	**0.0006**	**0.8239**	**No**	**No**	**0.0087**
Stephenville	**2.4956**	**Yes (+)**	**Yes (+)**	**0.5971**	**2.0764**	**Yes (+)**	**Yes (+)**	**0.0147**	**1.8002**	**No**	**Yes (+)**	**0.0110**	**2.3859**	**Yes (+)**	**Yes (+)**	**0.0009**	**2.3097**	**Yes (+)**	**Yes (+)**	**0.0178**

3.4.3 MK and Sen's slope analysis

MK and Sen's slope analysis results for monthly total PPT, monthly averaged max and min temperatures, monthly averaged modified HS and monthly averaged total water balance is given in Table 3-4. Trend calculations by the MK test for total monthly PPT, max and min temperatures, modified HS, and total water balance was somewhat in agreement with ITA and LOWESS analysis results. Trend indications of each studied parameter are given individually as follows.

Gander had positive PPT trends for both 90% and 95% confidence levels (CL) and *Stephenville* bared positive PPT trends for 90% CL, where all the other study locations showed no trend indication for May. June and August also indicated no trends for PPT for any of the locations. Only *Gander* had positive trends for both CL in July, and *St John's* had a positive trend at 90% CL. The remaining locations indicated no trend for July. Only *Port Aux Basque* and *St John's* showed a no trend of PPT for both CL in September. Additionally, *Deer Lake* bared no trend at 95% CL in September as well. In October only *Corner Brook* and *Stephenville* had positive PPT trends at 95% and 90% CL, whereas *Cormack* and *Cow Head* also had increasing PPT trends only at 90% CL.

Max temperature yielded positive trends in August at both 95% and 90% CLs for all locations. Whereas in July, only *Gander* showed no trend for both CLs and *St John's* also had no trend indication at 95% CL. *Port Aux Basque* was the only station that indicated a positive trend in June at 95% CL, while only *Corner Brook, Cow Head,* and *Stephenville* had positive trends at 90% CL. Positive trends in May only resulted in *Corner Brook, Deer Lake, Port Aux Basque* and *Stephenville*. While *Cormack* indicated no trend for September, all other locations had positive maximum temperature trends at 90% CL. In October *Cormack* behaved similar to that of September. Additionally, *Cow Head* also remained having no trend for September.

Min temperature held no trend cases in most of the locations and months. Only *Port Aux Basque* indicated having a positive trend through May to October, whereas *Corner Brook* had positive trends from June to October. In August and September, all locations had a positive trend except *Cow Head* and *Deer Lake*. Furthermore, apart from *Cow Head* and *Deer Lake*, *Cormack* did not have any trend in October.

Modified HS trends for May, June and August behaved similarly to maximum temperature trends of the respective months. In July, while the other locations indicated positive trends, only *Gander* and *St John's* showed no trend. Apart from *Cormack* and *Corner Brook*, the rest of the locations showed positive trends for September. Where only *Deer Lake*, *Port Aux Basque* and *Stephenville* had the only positive trends for October. Concerning total water balance, May June and August months had no trend for all locations studied. Only *Gander* indicated a significant positive trend for July, which followed the PPT trend pattern of July. September was characterised with positive trends for total water balance in *Cormack, Corner Brook, Cow Head*, *Gander* and *Stephenville*. *Cormack*, *Corner Brook* and *Stephenville* were the only locations which had increasing total water balance trends for October.

In general, for almost all locations and all parameters, i.e., total monthly PPT, monthly averaged max and min temperatures, modified HS, and total water balance; increasing trends were found within August, September, and October, which was a noticeable feature in this study. With respect to PPT, the results of this study contradicted that of Partal & Kahya, (2006), who showed that strong negative PPT trends were available throughout Turkey during September. Yue & Hashino, (2003) stated that PPT trends decreased throughout several regions of Japan in September, which was also contrary to the outcome of this study. This study also contradicted the results of Gajbhiye et al., (2016), where positive PPT trends were found throught out Sindh river basin, India in August. However, this study aligned with the results of

a study carried out in the hilly states of India, where there were positive PPT trends in September among other months (Yadav et al., 2014). Additionally this study aknowlages Akinremi et al., (1999), where they have stated the PPT, especially rainfall in the Canadian prairies have increased due to climate change, and state the PPT might be increasing due to climate chage effects over NL as well.

This study outlines that min and max temperature trends are can be found throughout the growing season, but are more focused within August and September months of NL, which contradicted the findings of Bonsal et al., (2001), as they emphasised, based on data analysis from 1950-98, that increments in temperature were focused on winter and spring over Canada. The study results somewhat aligned with the results of Cui et al., (2017), where they have stated, max and min temperatures had positive trends for Yangtze river basing over autumn seasons 1960-2015. This study also agreed with Clark er al., (2000), where they reported increase over time in temperature in Toronto, Ontario, Moncton, New Brunswick, and Indian Head, Saskatchewan. The results of Mohsin & Gough, (2010) pointed out increasing trends of temperature over Grater Toronto area particularly in winter, of which the results of this study were contradictary to the time period of the increasing trends.

Similar to max and min temperature patterns, modified HS also showed inceeasing trend patterns more focused within the months of August and September. These results agreed with Dinpashoh et al., (2018), where they stated that strong increasing trends in PET was found in Kermanshah station, Iran within the month of August. Although this study results somewhat agreed with the results of Sonali and Nagesh Kumar, (2016), where they illustrated that prominent PET trends in post-monsoon (October to December) for certain ares of India.

3.4.4 Comparison of trend analysis methods

To compare all trend results (significant and insignificant) from the two methods, a centred scatter plot was created to show ITA's D value versus MK's Z value (Figure 3-19), (Wu & Qian, 2017). The scatter plot exhibited that most of the points fell into the first and third quadrants, viz: in PPT 81.25%, in max and min temperatures 97.92% each and in modified HS 95.83%, which indicated the general trend agreement among methods. However, water balance trends detected by each method do not seem to agree with each other strongly since only 60.42% falls within the first and the third quadrants, and 8.33% falls under the second quadrant, and 31.25% falls under the fourth quadrant.

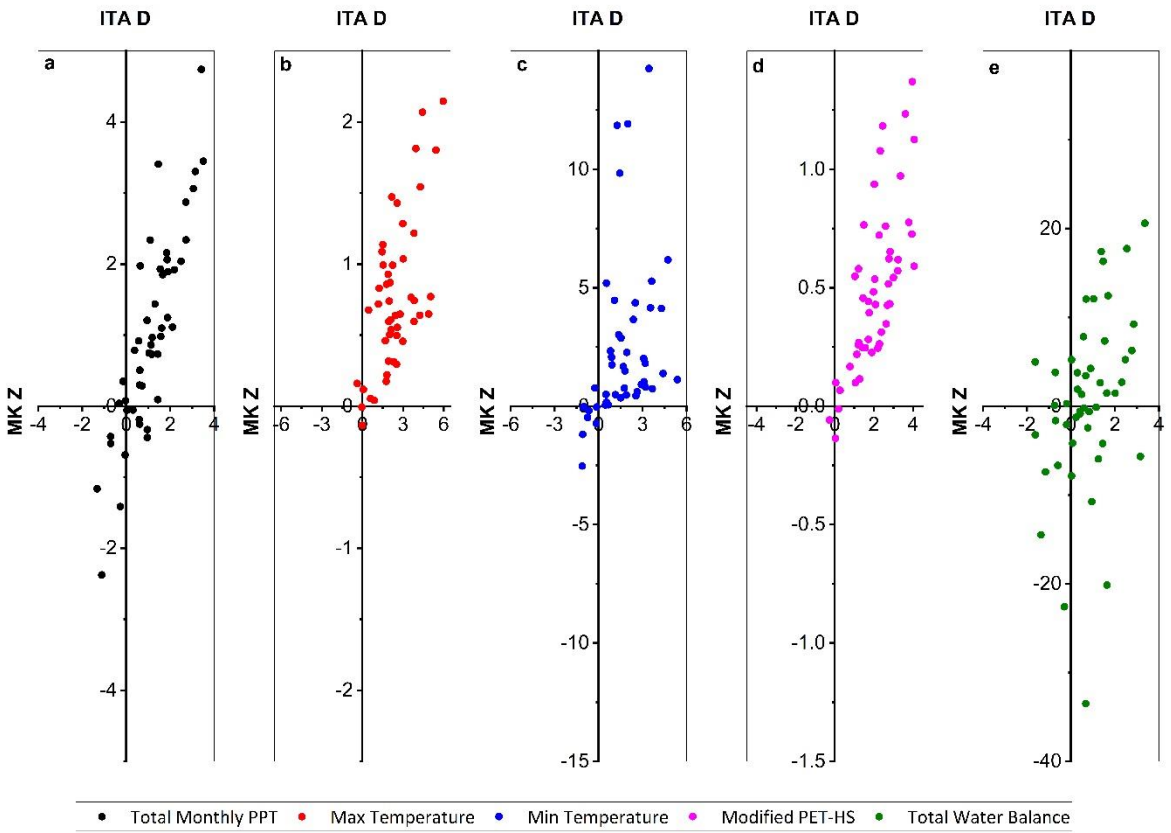

Figure 3-19: Scatter plots showing Z value of the Mann-Kendall test versus D value of ITA a: PPT, b: max, c: min Temp, d: PET and d: water balance.

3.5 Conclusion

From MK and ITA tests, it was possible to state that results from both tests agreed with each other for parameters; PPT, max and min temperatures and PET trends. This indicated that ITA is a reliable method to be used in trend identification, with the ability to identify trends more clearly both in graphical and statistical aspects. The trend calculation of total water balance by MK and ITA did not agree with each other in a high degree, where only 60.42% fell within the first and third quadrants. Unlike ITA, MK test can only detect monotonic trends (Kisi & Ay, 2014; Şen, 2012). It has difficulty in identifying positive and negative trends that are present in the same time series. Even though total water balance was calculated as the difference of PPT and PET, there may have been positive and negative trend variations within a selected time series of total water balance. And these variations might not have been captured by an MK test, hence the lower level of agreement between MK Z and ITA D for total water balance.

Against this background, it was possible to conclude that based on both ITA and MK tests, positive trends can be found throughout all locations and all months in PPT, max and min temperatures and PET. As for total water balance, most significant trends ranging from 0.018-0.076 mm/month/year was seen in September and October for most locations, where the other months considered did not have significant trends. Concerning PPT, significant increasing trends of magnitudes 0.375-2.210 mm/month/year were found for September and October. It was possible to note that total water balance followed PPT trend pattern in most locations. Both max and min temperatures indicated significant trends ranging within 0.015-0.062 ^{o}C/month/year for the entire growing season, especially within August and September in almost all locations. PET trends patterns closely followed max and min temperatures where the increments were up to 0.011 mm/month/year. In conclusion, it can be said that NL is also affected by the global climate change as reflected by the trend analysis carried out in this study.

The increasing PPT, PET and total water balance trend indications imply that better maintained water management systems are required for the NL agriculture industry and achieving the food security targets. Positive temperature trend indications suggest that NL may be able to gradually expand the length of the growing periods with respect to both timing and length in future as well.

Almost all locations indicating positive trends being concentrated within the later three months of the growing season for all studied hydrometeorological parameters is a noticeable occurrence, which urges the necessity for further detailed study of NL, focusing on August, September and October. Eventhough the results of this research may not completely agree with studies carried out throughout other regions of the world, on the specific time period of trend indications of each parameter, in a more broader context this study completely agrees to the fact that there are increasing trends throughout the world, and the main reason might be the influence of the climate change on the hydrologic regime.

As a progressive step of this research, the author would like to recommend future projection of trends in the parameters discussed above, using relatively new but highly accurate methods such as wavelet-transformed artificial neural network methods to facilitate reliable and sound decision making in the field of agriculture of NL.

3.6 References

Akinremi, O. O., McGinn, S. M., & Cutforth, H. W. (1999). Precipitation trends on the Canadian prairies. *Journal of Climate*, *12*(10), 2996-3003.

Bonsal, B. R., Zhang, X., Vincent, L. A., & Hogg, W. D. (2001). Characteristics of daily and extreme temperatures over Canada. *Journal of Climate*, *14*(9), 1959-1976.

Brandt, J. P. (2009). The extent of the North American boreal zone. *Environmental*

Reviews, *17*(NA), 101-161.

Caloiero, T. (2017). Trend of monthly temperature and daily extreme temperature during 1951–2012 in New Zealand. *Theoretical and Applied Climatology*, *129*(1), 111-127.

Chandler, R., & Scott, M. (2011). *Statistical methods for trend detection and analysis in the environmental sciences*. John Wiley & Sons.

Clark, J. S., Yiridoe, E. K., Burns, N. D., & Astatkie, T. (2000). Regional climate change: trend analysis of temperature and precipitation series at selected Canadian sites. *Canadian Journal of Agricultural Economics/Revue Canadienne D'agroeconomie*, *48*(1), 27-38.

Cui, L., Wang, L., Lai, Z., Tian, Q., Liu, W., & Li, J. (2017). Innovative trend analysis of annual and seasonal air temperature and rainfall in the Yangtze River Basin, China during 1960–2015. *Journal of Atmospheric and Solar-Terrestrial Physics*, *164*, 48-59.

Dinpashoh, Y., Jahanbakhsh-Asl, S., Rasouli, A. A., Foroughi, M., & Singh, V. P. (2019). Impact of climate change on potential evapotranspiration (case study: west and NW of Iran). *Theoretical and Applied Climatology*, *136*(1), 185-201.

Duhan, D., & Pandey, A. (2013). Statistical analysis of long term spatial and temporal trends of precipitation during 1901–2002 at Madhya Pradesh, India. *Atmospheric Research*, *122*, 136-149.

Environment and Climate Change Canada. (2020). Historical Data. Retrieved February 4, 2020, from https://climate.weather.gc.ca/historical_data/search_historic_data_e.html

Fernandes, R., Korolevych, V., & Wang, S. (2007). Trends in land evapotranspiration over Canada for the period 1960–2000 based on in situ climate observations and a land surface model. *Journal of Hydrometeorology*, *8*(5), 1016-1030.

Fu, G., Yu, J., Yu, X., Ouyang, R., Zhang, Y., Wang, P., ... & Min, L. (2013). Temporal variation of extreme rainfall events in China, 1961–2009. *Journal of Hydrology, 487*, 48-59.

Gajbhiye, S., Meshram, C., Mirabbasi, R., & Sharma, S. K. (2016). Trend analysis of rainfall time series for Sindh river basin in India. *Theoretical and Applied Climatology, 125*(3), 593-608.

Ghilain, N. (2016). Continental Scale Monitoring of Subdaily and Daily Evapotranspiration Enhanced by the Assimilation of Surface Soil Moisture Derived from Thermal Infrared Geostationary Data. In *Satellite Soil Moisture Retrieval* (pp. 309-332). Elsevier.

Katul, G., & Novick, K. (2009). Evapotranspiration. *Encyclopedia of Inland Waters*, 661-667.

Kendall, M. G. Rank Correlation Methods; Griffin: London, UK, 1975.

Khaliq, M. N., Ouarda, T. B., Gachon, P., Sushama, L., & St-Hilaire, A. (2009). Identification of hydrological trends in the presence of serial and cross correlations: A review of selected methods and their application to annual flow regimes of Canadian rivers. *Journal of Hydrology, 368*(1-4), 117-130.

King, M., Altdorff, D., Li, P., Galagedara, L., Holden, J., & Unc, A. (2018). Northward shift of the agricultural climate zone under 21st century global climate change. *Scientific Reports, 8*(1), 1-10.

Kisi, O. (2015). An innovative method for trend analysis of monthly pan evaporations. *Journal of Hydrology*, *527*, 1123-1129.

Kisi, O., & Ay, M. (2014). Comparison of Mann–Kendall and innovative trend method for water quality parameters of the Kizilirmak River, Turkey. *Journal of Hydrology, 513*,

362-375.

Kişi, Ö., Guimaraes Santos, C. A., Marques da Silva, R., & Zounemat-Kermani, M. (2018). Trend analysis of monthly streamflows using Şen's innovative trend method. *Geofizika*, *35*(1), 53-68.

Kumar, N., Panchal, C. C., Chandrawanshi, S. K., & Thanki, J. D. (2017). Analysis of rainfall by using Mann-Kendall trend, Sen's slope and variability at five districts of south Gujarat, India. *Mausam*, *68*(2), 205-222.

Larsen, J. A. (2013). *The boreal ecosystem*. Elsevier.

Lim, C. F. A., Suzuki, M., Ohte, N., Hotta, N., & Kume, T. (2009). Evapotranspiration patterns for tropical rainforests in Southeast Asia: a model performance examination of the Biome-BGC model. *Bulletin of the Tokyo University Forests*, *120*, 29-44.

Mann, H. B. (1945). Nonparametric tests against trend. *Econometrica: Journal of the Econometric Society*, 245-259.

Mehan, S., Kannan, N., Neupane, R. P., McDaniel, R., & Kumar, S. (2016). Climate change impacts on the hydrological processes of a small agricultural watershed. *Climate*, *4*(4), 56.

Mohorji, A. M., Şen, Z., & Almazroui, M. (2017). Trend analyses revision and global monthly temperature innovative multi-duration analysis. *Earth Systems and Environment*, *1*(1), 1-13.

Mohsin, T., & Gough, W. A. (2010). Trend analysis of long-term temperature time series in the Greater Toronto Area (GTA). *Theoretical and Applied Climatology*, *101*(3), 311-327.

Öztopal, A., & Şen, Z. (2017). Innovative trend methodology applications to precipitation records in Turkey. *Water Resources Management*, *31*(3), 727-737.

Park, C. E., Jeong, S. J., Joshi, M., Osborn, T. J., Ho, C. H., Piao, S., ... & Feng, S. (2018). Keeping global warming within 1.5 C constrains emergence of aridification. *Nature Climate Change*, *8*(1), 70-74.

Partal, T., & Kahya, E. (2006). Trend analysis in Turkish precipitation data. *Hydrological Processes: An International Journal*, *20*(9), 2011-2026.

Pohlert, T. (2020). trend: non-parametric trend tests and changepoint detection.–R package ver. 1.1. 2.

Prăvălie, R., Piticar, A., Roșca, B., Sfîcă, L., Bandoc, G., Tiscovschi, A., & Patriche, C. (2019). Spatio-temporal changes of the climatic water balance in Romania as a response to precipitation and reference evapotranspiration trends during 1961–2013. *Catena*, *172*, 295-312.

Sen, P. K. (1968). Estimates of the regression coefficient based on Kendall's tau. *Journal of the American Statistical Association*, *63*(324), 1379-1389.

Şen, Z. (2012). Innovative trend analysis methodology. *Journal of Hydrologic Engineering*, *17*(9), 1042-1046.

Şen, Z. (2017). Innovative trend significance test and applications. *Theoretical and Applied Climatology*, *127*(3-4), 939-947.

Senay, G. B., Velpuri, N. M., Bohms, S., Budde, M., Young, C., Rowland, J., & Verdin, J. P. (2015). Drought monitoring and assessment: remote sensing and modeling approaches for the famine early warning systems network. In *Hydro-meteorological hazards, risks and disasters* (pp. 233-262). Elsevier.

Sonali, P., & Nagesh Kumar, D. (2016). Spatio-temporal variability of temperature and potential evapotranspiration over India. *Journal of Water and Climate Change*, *7*(4), 810-822.

Szilagyi, J., & Jozsa, J. (2018). Evapotranspiration trends (1979–2015) in the Central Valley of California, USA: Contrasting tendencies during 1981–2007. *Water Resources Research*, *54*(8), 5620-5635.

Tabari, H., Marofi, S., Aeini, A., Talaee, P. H., & Mohammadi, K. (2011). Trend analysis of reference evapotranspiration in the western half of Iran. *Agricultural and Forest Meteorology*, *151*(2), 128-136.

Taylor, S. J., Ferguson, J. H. W., Engelbrect, F. A., Clark, V. R., Van Rensburg, S., & Barker, N. (2016). The Drakensberg Escarpment as the great supplier of water to South Africa. Elsevier.

Tosunoglu, F., & Kisi, O. (2017). Trend analysis of maximum hydrologic drought variables using Mann–Kendall and Şen's innovative trend method. *River Research and Applications*, *33*(4), 597-610.

Wu, H., & Qian, H. (2017). Innovative trend analysis of annual and seasonal rainfall and extreme values in Shaanxi, China, since the 1950s. *International Journal of Climatology*, *37*(5), 2582-2592.

Yadav, R., Tripathi, S. K., Pranuthi, G., & Dubey, S. K. (2014). Trend analysis by Mann-Kendall test for precipitation and temperature for thirteen districts of Uttarakhand. *Journal of Agrometeorology*, *16*(2), 164.

Yue, S., & Hashino, M. (2003). Long term trends of annual and monthly precipitation in Japan 1. *JAWRA Journal of the American Water Resources Association*, *39*(3), 587-596.

Zhang, K., Kimball, J. S., Mu, Q., Jones, L. A., Goetz, S. J., & Running, S. W. (2009). Satellite based analysis of northern ET trends and associated changes in the regional water balance from 1983 to 2005. *Journal of Hydrology, 379*(1-2), 92-110.

Zhang, Q., Xu, C. Y., Chen, Y. D., & Ren, L. (2011). Comparison of evapotranspiration variations between the Yellow River and Pearl River basin, China. *Stochastic Environmental Research and Risk Assessment, 25*(2), 139-150.

Chapter 4: General Conclusion and Recommendations

It was possible to conclude that the temperature-based Hargreaves-Samani (HS) equation was acceptable to calculate potential evapotranspiration (PET) for Newfoundland (NL). The further modified HS can be applied to calculate PET specifically during the growing season for study locations of *Cormack*, *Corner Brook*, *Deer Lake* and *Gander*. For other locations, namely, *Cow Head*, *Port Aux Basque* and *Stephenville*, the same modified equation could be used with error margins of 0.072, 0.055 and 0.071 mm/day respectively. This modified HS can be used with reasonable accuracy when PET calculations are needed in Newfoundland for decisions on agricultural water management, cropping systems, integrated watershed management, water balance and hydrological modelling etc.

Mann-Kendal (MK) and Innovative Trend Analysis (ITA) test result comparison indicated both tests agreed with each other for parameters: total monthly precipitation (PPT), maximum (max) and minimum (min) temperatures and PET trends. Therefore, ITA can be considered as a reliable method to be used in trend identification, with the ability to identify trends more clearly both graphically and statistically. Even though ITA was able to identify the clear positive and negative trends, the variation between having positive and negative trends in the same time series may have affected MK test to identify trends of water balance, since MK test can only detect monotonic trends. In conclusion, based on both ITA and MK tests, positive trends could be found throughout all locations and all months in PPT, max and min temperatures and PET. As for total water balance, most of the significant trends ranging from 0.018-0.076 mm/month/year could be seen in September for most locations. Significantly increasing PPT trends of magnitudes 0.375-2.210 mm/month/year were found for September and October. In almost all locations, max and min temperatures indicated significant positive trends ranging within 0.015-0.062 ºC/month/year throughout the entire growing season. Having increasing

trends of both min and max temperatures concentrated within August and September was a notable feature. PET trends closely followed that of max and min temperatures where the increments up to 0.011 mm/month/year.

The results of these studies have achieved the study objectives by successfully recommending an empirical equation and further modifying it to calculate PET accurately for the growing season in NL, and identifying existing trends associated with PPT, max and min temperatures, PET and total water balance for the growing season in NL. A comparative study of real-time measured PET data with remote sensing-based inputs and based water balance prediction is advised as a recommendation to the continual of this study. Furthermore, Future projection of trends in the parameters discussed above using relatively new but highly accurate methods such as wavelet-transformed artificial neural network methods is encouraged as a progressive step of this research.

Appendices

5.1 Potential evapotranspiration calculation equations used

5.1.1 Makkink Equation (Lu et al., 2005; Zotarelli et al., 2010)

$$PET = 0.61\frac{1}{\lambda}\frac{\Delta Rs}{(\Delta + \gamma)} - 0.12$$

$$\lambda = 2.45$$

Rs = Solar radiation [MJ/m2/day]

Δ = slope of the saturation vapor pressure vs. temperature curve [kPa/ °C]

γ = Psychrometric constant [kPa/ °C]

5.1.2 Priestly and Taylor Equation (Lu et al., 2005; Zotarelli et al., 2010)

$$PET = \frac{1}{\lambda}\frac{\Delta(Rn - G)}{(\Delta + \gamma)}\alpha$$

λ = latent heat of vaporization = 2.45 [MJ/ kg]

α = Priestly Taylor coefficient

Δ = slope of the saturation vapor pressure vs. temperature curve [kPa/ °C]

Rn = net radiation flux at the surface [MJ/m^2/day]

G = the sensible heat exchange from the surface to the soil (positive if the soil is warming) [MJ/m^2/day]

γ = Psychrometric constant [kPa/ °C]

5.1.3 Hargreaves- Samani Equation (Lu et al., 2005; Zotarelli et al., 2010)

$$PET = 0.0023\frac{Ra}{\lambda}\ (T_{max} - T_{min})^{0.5}(T_{mean} + 17.8)$$

T_{mean} = average air temperature of the day (°C)

T_{max} = maximum Temperature of the day (°C)

T_{min} = minimum Temperature of the day (°C)

Ra = extraterrestrial radiation [MJ/m^2/day]

5.1.4 Turc Equation (Zotarelli et al., 2010; Lu et al., 2005)

$$PET = 0.0133 \frac{Tmean}{Tmean+15} (23.8856Rs + 50)$$

T_{mean} = average air temperature (°C)

Ra = extraterrestrial radiation [MJ/m^2/day]

5.1.5 Hamon Equation (Lu et al. 2005).

$$PET = 0.1651(Ld)(RHOSAT)(KPEC)$$

$$RHOSAT = 216.7\ x\ \frac{ESAT}{(T_{mean} + 237.3)}$$

$$ESAT = 6.108\ x \exp\ [(17.26939\ x\ (T_{mean})/(T_{mean} + 237.3)]$$

Ld = daytime length (h)

RHOSAT is the saturated vapour density (g/m3)

KPEC = calibration coefficient = 1.2

T_{mean} = daily mean air temperature

ESAT = Saturated vapour pressure at a given temperature. In this case T_{mean}